Tuomas Mutanen

Brain state dynamics in transcranial magnetic stimulation—A combined TMS–EEG study

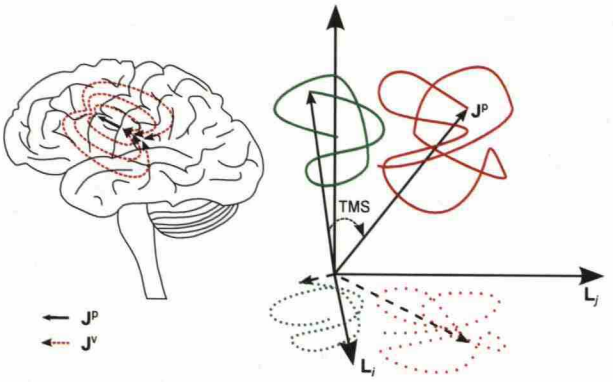

School of Science

Thesis submitted for examination for the degree of Master of Science in Technology.

Espoo 12th of August 2013

Thesis supervisor:

Prof. Risto J. Ilmoniemi

Thesis advisor:

Jaakko O. Nieminen, Ph.D.

Aalto University
School of Science

AALTO-YLIOPISTO
PERUSTIETEIDEN KORKEAKOULU

DIPLOMITYÖN
TIIVISTELMÄ

Tekijä: Tuomas Mutanen

Työn nimi: Aivotilan dynamiikka käytettäessä transkraniaalista magneettistimulaatiota: yhdistetty TMS–EEG-tutkimus

Päivämäärä: 12.8.2013 Kieli: Englanti Sivumäärä: 6+48

Lääketieteellisen tekniikan ja laskennallisen tieteen laitos

Professuuri: Teknillinen fysiikka Koodi: Tfy-99

Valvoja: Prof. Risto J. Ilmoniemi

Ohjaaja: TkT Jaakko O. Nieminen

Yhdistettyä transkraniaalista magneettistimulaatiota (TMS) ja aivosähkökäyrää (EEG) on käytetty menestyksekkäästi tutkittaessa aivojen konnektiivisuutta ja reaktiivisuutta. TMS:n vaikutuksia käynnissä olevaan aivotoimintaan ei kuitenkaan tunneta kovin hyvin suurelta osalta siksi, että nykyiset tavat analysoida TMS–EEG-signaalia kuvaavat useimmiten ennemminkin keskiarvovastetta kuin TMS:n aiheuttamia välittömiä muutoksia.

Tämän diplomityön tarkoituksena on pyrkiä ymmärtämään TMS:n dynamiikkaa analysoimalla EEG:tä. Tärkeimpänä tavoitteena on selvittää kuinka TMS vaikuttaa aivojen tilaan ja toisaalta kuinka TMS:ää edeltävä aivojen tila muuttaa TMS:n vaikutuksia. Aiheen syvällisempi ymmärrys on tärkeää kehitettäessä hienostuneempia ja tehokkaampia stimulaatiosarjoja sekä -tapoja.

Esittelemme tässä diplomityössä kaksi uutta kvantitatiivista työkalua nimiltään keskimääräinen tilamuutos (MSS) sekä tilavarianssi (SV) ja näytämme, että ne kykenevät mittaamaan TMS:n hetkellisiä vaikutuksia aivojen sähköiseen tilaan. Suoritimme myös mittauksia, joissa aivotilaa muutettiin ennen varsinaista TMS-testipulssia ja näytämme, että tämä modulaatio vaikuttaa TMS:n jälkeiseen EEG-signaaliin. Lisäksi ryhmätason tulokset viittaavat siihen, että stimulaation aiheuttamat muutokset MSS:ssä ja SV:ssä ovat herkkiä TMS:ää edeltävälle aivotilalle.

Avainsanat: Transkraniaalinen magneettistimulaatio, Aivosähkökäyrä, Dynamiikka, Aivotila

AALTO UNIVERSITY
SCHOOL OF SCIENCE

ABSTRACT OF THE
MASTER'S THESIS

Author: Tuomas Mutanen

Title: Brain state dynamics in transcranial magnetic stimulation—A combined TMS–EEG study

Date: 12th of August 2013 Language: English Number of pages: 6+48

Department of Biomedical Engineering and Computational Science

Professorship: Engineering physics Code: Tfy-99

Supervisor: Prof. Risto J. Ilmoniemi

Advisor: Jaakko O. Nieminen, Ph.D.

Transcranial magnetic stimulation (TMS) and electroencephalography (EEG) have been successfully combined to study the connectivity and reactivity of the brain. However, it is not yet well understood how TMS modulates the ongoing brain activity largely because the present methods used to analyze TMS–EEG signals usually describe the average response to TMS rather than the immediate effects.

The purpose of this Thesis is to improve our understanding on the dynamics of TMS by analyzing EEG signals; How does TMS affect the state of the brain, and on the other hand, how does the state of the brain change the effects of TMS? Deeper understanding on this subject is vital when seeking for more elaborate and effective stimulation sequences and methods.

In this Thesis, we introduce two quantitative tools called mean state shift (MSS) and state variance (SV) and show that they are able to quantify the transient effects of TMS on the electric brain state. Furthermore, by performing measurements where the state of the brain was modulated before the actual test TMS pulse we show that this state modulation affects post-TMS EEG. Furthermore, the group-level results imply that the TMS-elicited changes in MSS and SV are sensitive to the pre-TMS state modulation.

Keywords: Transcranial magnetic stimulation, Electroencephalography, Dynamics, Brain state

Preface

I want to thank our whole TMS research group but especially my supervisor Risto Ilmoniemi and instructor Jaakko Nieminen for their valuable comments and help in general. Without their support, advice, and encouragement I could not have achieved the same quality in my work.

This Master's thesis is based on the work started in January 2013. Thus, parts of the theory, results, and discussion presented in this work have already been published in Frontiers of Human Neuroscience (Mutanen et al., 2013) with slight differences.

Tuomas Mutanen
Otaniemi, 12th of August 2013

Contents

List of Abbreviations

ADM	*Abductor digiti minimi*
APB	*Abductor pollicis brevis*
EEG	Electroencephalography
EMG	Electromyography
EMM	Energy measure of modulation
ERP	Event-related potential
eSV	Evoked state variance
GMFA	Global mean-field amplitude
ISI	Inter-stimulus interval
LICI	Long-interval intracortical inhibition
M1	Primary motor cortex
MEG	Magnetoencephalography
MEP	Motor-evoked potential
MR	Magnetic resonance
MSS	Mean state shift
nTMS	Navigated TMS
RMS	Root mean square
RMT	Resting motor threshold
ROI	Region of interest
RQA	Recurrence quantification analysis
rTMS	Repetitive TMS
SEM	Standard error of the mean
SICF	Short-interval intracortical facilitation
SICI	Short-interval intracortical inhibition
SICM	Short-interval intracortical modulation
SSP	Signal space projection
SV	State variance
SVD	Singular value decomposition
TES	Transcranial electric stimulation
TMS	Transcranial magnetic stimulation

1 Introduction

Transcranial magnetic stimulation (TMS) is a method where the cortex is activated artificially by generating a short and strong magnetic pulse which induces an electric field inside the brain. Due to the electrophysiological properties of the brain tissue, the induced electric field activates targeted neurons after which secondary neural populations are excited through synaptic connections. Relatively recent technical development has enabled the measurement of electroencephalography (EEG) simultaneously with TMS. In EEG, several electrodes recording the potential differences across the head are attached on the subject's scalp. This allows us to study the time evolution of the TMS-evoked activity, since changes in post-synaptic currents ultimately lead to measurable potential differences.

Previous studies have shown that TMS changes the state of the brain. Much of the evidence can be found in the studies where TMS has been combined with electromyography (EMG). When TMS is applied to the primary motor cortex (M1), involuntary muscle activation can be seen in electrodes attached to the target muscle (Barker et al., 1985). Furthermore, several TMS–EMG results indicate that the TMS-evoked cortical activation is state-dependent; when researchers have been capable of reliably modifying the cortical excitability of the brain right before stimulation also the TMS–EMG responses have changed (*e.g.*, Valls-Solé et al., 1992; Claus et al., 1992; Kujirai et al., 1993).

Thus, when using TMS, the situation is dynamic. TMS changes the functioning of the studied brain; the observed changes depend on the current state of the brain at the moment of stimulus. Obtaining further understanding on these complex mechanisms is important when developing more elaborate and efficient stimulation sequences.

By combining EEG with TMS, one can measure more directly the modulation of the cortical state due to the TMS pulse, compared to solely looking the EMG response. Unfortunately, this has proven to be a challenging task. One reason for this is that TMS-elicited changes in the EEG signals are subtle compared to the total background activity (Mäki and Ilmoniemi, 2010). The conventional solution is to measure several trials of TMS-evoked responses and study their average. This effectively suppresses the background activity, highlighting the TMS-evoked response (*e.g.*, Komssi et al., 2004; Lioumis et al., 2009). However, the procedure does not allow studying the immediate effects of TMS.

Hence, the first goal of this Thesis is to introduce new EEG measures called mean state shift (MSS) and state variance (SV) that can be computed from trial-level data to quantify the changes from pre- to post-TMS brain activity. We validated these measures by applying them to data found in our database. Additionally, we tested the importance of signal quality when using MSS and SV by adding simulated noise into the studied datasets.

The second goal of this Thesis is to study how the cortical excitation level at the moment of stimulation affects the TMS–EEG signals. Hence, we performed additional measurements where we used the paired-pulse technique. There, the purpose of the first pulse is to either excite or inhibit the cortex before the second

pulse finalizes the activation. We tested whether the TMS-elicited modulation in MSS and SV would be different when the pre-TMS state is controlled and varied using the first pulse. We validated the observations by comparing the obtained results with more established EEG analysis tools, showing cortical facilitation or inhibition.

2 TMS-evoked EEG responses reflect the state of the brain

The fundamentals of TMS can be explained with Maxwell's equations (Ilmoniemi et al., 1999). According to the Biot–Savart law, a current $I(t)$ in a coil produces a magnetic field:

$$\mathbf{B}(\mathbf{r},t) = \frac{\mu_0}{4\pi} I(t) \oint_C \frac{d\mathbf{l}(\mathbf{r}') \times (\mathbf{r} - \mathbf{r}')}{|\mathbf{r} - \mathbf{r}'|^3}, \tag{1}$$

where $\mathbf{B}(\mathbf{r},t)$ is the time-varying magnetic field at location $\mathbf{r}$, μ_0 is the vacuum permeability, and $d\mathbf{l}$ is a differential wire element. On the other hand, Faraday's law states that a changing magnetic field induces an electric field $\mathbf{E}$:

$$\nabla \times \mathbf{E} = -\frac{\partial \mathbf{B}}{\partial t}. \tag{2}$$

When a strong current pulse peaking at ~5–10 kA in ~100 µs is driven through a typical TMS coil, which is placed on the scalp, the time derivative of the magnetic field induces an electric field with the strength of ~100 V/m in the cortex. Such an electric field is sufficient to depolarize axon membranes enough for the cells to launch action potentials. The level of depolarization depends on the axonal geometry with respect to the induced electric field. Especially axonal bends are depolarized, and hence activated (see Fig. 1).

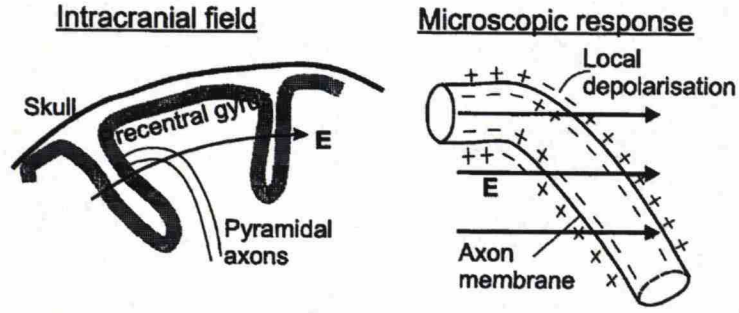

Figure 1: The physiological explanation for the cortical activation induced with TMS. When a TMS coil is placed so that the maximal induced electric field is perpendicular to a certain sulcus, primarily those pyramidal cells whose axons are bent with respect to the field are activated. Modified from Ilmoniemi et al. (1999).

The main benefit of TMS when compared to more conventional transcranial electric stimulation (TES) is that the skull is transparent for the magnetic field. In TES, two or more sponge electrodes are placed on the scalp with a voltage sufficient to drive a current through the insulating skull, and finally, through the brain. Hence, if no severe discomfort is wished to be caused to the subject, much larger electric fields can be generated in the brain by using TMS. However, the strength of the

magnetic field and induced electric field decay rapidly when moving away from the coil. Furthermore, in TMS, the maximum of the induced electric field is always on a conductive boundary (Heller and van Hulsteyn, 1992). In consequence, only the cortex can be primarily stimulated when using TMS. Nevertheless, TMS is able to activate also remote brain areas due to natural synaptic transmission of activity (Ilmoniemi et al., 1997; Komssi et al., 2002; Massimini et al., 2005).

Modern TMS coils usually consist of two coils adjacent to each other, a so-called figure-of-eight coil, producing a focal induced electric field in the cortex (see Fig. 2), which enables precise targeting of stimulation (Hannula et al., 2005). Nowadays, TMS is usually combined with neuronavigation (nTMS), which provides superior stimulation accuracy (Julkunen et al., 2009). In nTMS, infrared markers, whose positions can be monitored with a special camera, are attached to the subject's head and to the coil. By combining the information of the coil's position and orientation relative to the head and the magnetic resonance (MR) images of the subject, the researcher obtains accurate real-time information of the stimulation location in the cortex.

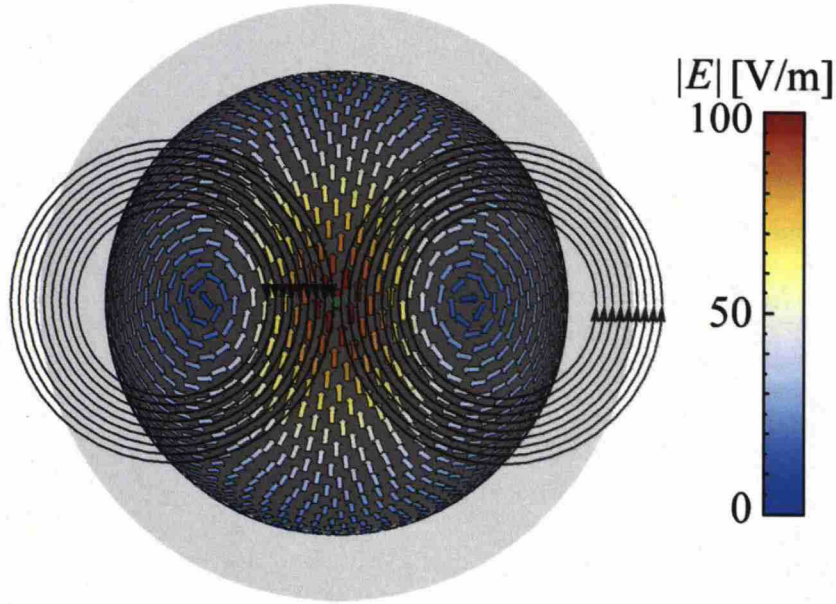

Figure 2: The induced electric field generated by a modern figure-of-eight coil in a spherical head model. The maximal electric field is focal and locates directly under the middle point of the adjacent coil loops. Modified from Koponen (2012).

Another significant improvement, in addition to nTMS, was the introduction of a TMS-compatible EEG system that does not get saturated by the strong magnetic pulses (Virtanen et al., 1999). Combination of nTMS with TMS-compatible EEG provides a tool that allows precise and accurate artificial activation of the brain with simultaneous recording of the brain activity. EEG enables us to analyze TMS-modulated brain activity with good temporal resolution (~1 ms). However, the

spatial resolution of EEG is moderate ($\sim$1 cm^3 or more depending on the location) (Malmivuo et al., 1997) due to the poorly known conductivity properties. With EEG, better spatial resolution is difficult to achieve due to the conductivity properties of the skull and scalp, which affect the potential patterns created by the brain activity. Nevertheless, recent years have proven TMS–EEG to be a valuable method in understanding the connectivity and reactivity of the brain (*e.g.*, Ilmoniemi et al., 1997; Massimini et al., 2005; Huber et al., 2013). In this Thesis, we use combined nTMS–EEG with a figure-of-eight-coil.

2.1 Connection between the brain state and TMS–EEG

The current distribution $\mathbf{J}(\mathbf{r}, t)$ in the brain is often expressed in two parts:

$$\mathbf{J}(\mathbf{r}, t) = \mathbf{J}^{\mathrm{P}}(\mathbf{r}, t) + \mathbf{J}^{\mathrm{V}}(\mathbf{r}, t)\,, \tag{3}$$

where $\mathbf{J}^{\mathrm{P}}$ is the primary current density arising from the bioelectric activation of neurons (*e.g.*, post-synaptic currents), $\mathbf{J}^{\mathrm{V}}$ is the volume current density, $\mathbf{r}$ is the position, and t is the time.

While $\mathbf{J}^{\mathrm{V}}$ is a passive, ohmic current density driven by $\mathbf{J}^{\mathrm{P}}$ (Malmivuo and Plonsey, 1995) (Fig. 3 A), $\mathbf{J}^{\mathrm{P}}$ can be thought of as the primary source creating all the current density, which in turn affects the charge distribution that defines the electric potential. Hence, the EEG signal, *i.e.*, the voltage, measured by channel j can be expressed as

$$x_j(t) = \int \mathbf{L}_j(\mathbf{r}') \cdot \mathbf{J}^{\mathrm{P}}(\mathbf{r}', t) dv'\,, \tag{4}$$

where $\mathbf{L}_j(\mathbf{r})$ is the lead field determined by the geometry of the measurement set-up and the conductivity of the head (Ilmoniemi and Kičić, 2010). In other words, $\mathbf{L}_j(\mathbf{r})$ describes how efficiently channel j detects primary current at $\mathbf{r}$.

Thus, EEG can be considered the measurement of the projection of the primary current density on the signal space, the projection being defined by the lead fields of the channels. Since the primary current density describes accurately the electric state of the brain, EEG signals can be considered projections of the electric brain state. As $\mathbf{J}^{\mathrm{P}}(\mathbf{r}, t)$, *i.e.*, the state of the brain, changes, it draws a trajectory in the multidimensional state space. The trajectory is also projected on the EEG signal space (Fig. 3 B). The conventional method of analyzing one EEG channel of interest separately means that only the projection of the brain state on this particular channels will affect the results.

On the other hand, TMS can be used to modulate $\mathbf{J}^{\mathrm{P}}$. In the brain, the changing magnetic field induces an electric field which elicits action potentials in the axons. When action potentials reach synapses, post-synaptic currents that are visible in the EEG signals are created.

Our hypothesis is that TMS moves the brain higher in the energy landscape (here the energy landscape describes the tendency of the system to go from low-probability to high-probability states; from high energy to low energy) reflecting the information processing system. Hence, the TMS-modulated activity at the stimulation site is seen in the brain state trajectory as a sudden shift to a new region in the state

space (Fig. 3 B), which would be spontaneously occupied with smaller probability. We test this hypothesis directly by measuring MSS[1] which quantifies the mean distance between the brain states from two different time intervals. According to the hypothesis, it is expected that, due to TMS, there is a transient increase in MSS with respect to the baseline.

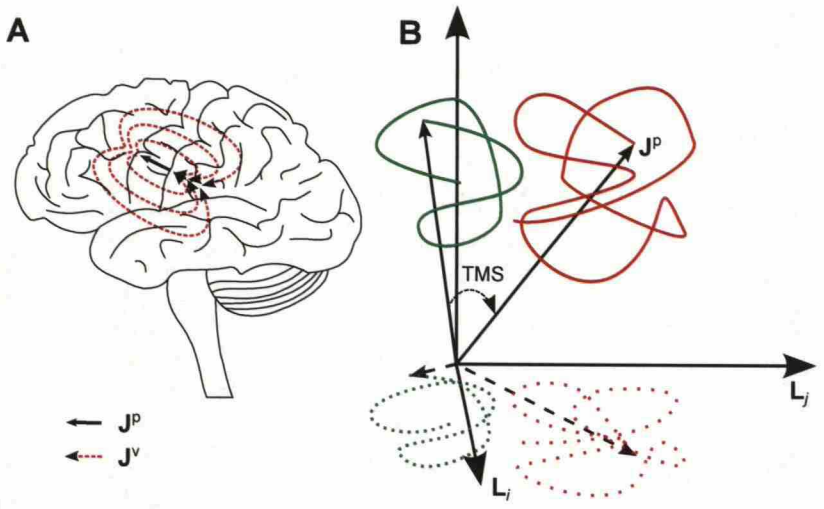

Figure 3: (A) The black arrow represents one primary current source, a flow of ions in synapses in the left M1. The dashed red lines represent the returning volume current. $\mathbf{J}^{\mathrm{P}}(\mathbf{r})$ describes the whole primary current distribution in the brain. (B) A schematic image of the hypothesis concerning the effect of TMS on the brain state. The green and red curves correspond to pre- and post-TMS brain-state trajectories, respectively. The spontaneous activity draws a trajectory in a certain region until TMS shifts the brain state to a new region in the state space. Furthermore, the brain state fluctuates more after TMS because of the increased free energy until the state gradually returns to the original set of spontaneous states. The projection of these effects can be seen in the EEG signal space, which is spanned by channels i and j. In the signal space, the trajectories are measured only at discrete time points, which is emphasized with dotted curves. This figure was originally published in Mutanen et al. (2013).

If the state of the brain is higher in the energy landscape, there is more free energy for the brain to act. The brain tends to minimize the free energy and get closer to some local energy minimum leading to enhanced fluctuation after TMS. This fluctuation is quantified using SV[1], which gives the variance of the signal vector during a studied time interval. According to the hypothesis, SV is expected to be increased until the system is closer to spontaneously probable states.

If the changes in the trajectory due to a single TMS pulse are large enough, they could also be visible in the obtained EEG signals. Since EEG is a low-dimensional

[1]See Section 3.3.2 for the exact definition.

projection of the original primary current distribution, any significant difference between the signal vectors also indicates a difference in the original state vectors.

Since the brain is a dynamic system whose future states, *i.e.*, trajectory, are dependent on its present state (as well as sensory input), it can be expected that also TMS responses depend on the present state. For instance, when active, certain inhibitory neuronal populations might decrease the TMS-evoked activity (Nikulin et al., 2003), and hence also TMS-elicited state shift among the subsequent fluctuation. On the other hand, if excitatory inputs are active at the moment of a TMS pulse, the effect could be more pronounced.

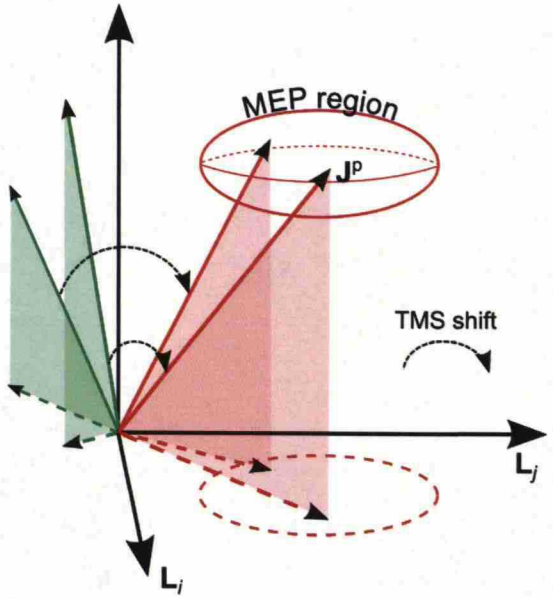

Figure 4: A schematic image representing the idea of TMS driving brain to a state of generating a MEP. The figure shows two separate TMS trials. The two green vectors correspond to pre-TMS and the red vectors to post-TMS states. In the state space, there is a region of states capable of launching a MEP. This is probably still a huge subsample but, anyhow, significantly smaller when compared to the collection of all possible brain states. If the stimuli are given with such parameters that the probability of TMS-evoked MEPs is larger, TMS would be capable of shifting the brain even from remote states to the MEP region. This should be visible in the average MSS in different conditions.

When stimulating the M1, it is possible to measure motor-evoked potentials (MEPs) that reflect cortical activation with electrodes attached to peripheral muscles. Hence, when stimulating the M1, more effective stimulation would mean more and stronger MEPs. If we assume that the states that launch a MEP are relatively close to each other in the state space and that the spontaneous brain state before the stimulus can wander relatively freely in the state space, the increased MEP probability should result in a larger average MSS (see Fig. 4). Furthermore, it is reasonable to expect that when large MEPs are measured, post-TMS state region is

even more restricted, since less brain states are capable of producing such large MEPs, further increasing MSS. Again, the increase in MSS is expected to also increase SV after the pulse.

For testing the latter part of the hypothesis, we performed measurements where the state of the brain was controlled using two different conditioning pulses before a test pulse. Finally, we computed MSS and SV in one control and two modulated conditions.

2.2 Previous studies showing state dependence of TMS–EEG responses

TMS–EEG has proven to be a useful tool in quantifying the effects of brain state on brain responses. For instance, several studies have probed the effect of sleep on the brain with TMS–EEG. Massimini et al. (2005) showed that during sleep the spatiotemporal features of the TMS-evoked EEG responses are changed. Later studies indicate that also different sleep stages induce measurable changes in TMS–EEG responses (Ferrarelli et al., 2010; Massimini et al., 2010). On the other hand, Huber et al. (2013) showed that prolonged wakefulness increases cortical excitability, which was quantified by measuring the amplitudes of the early-latency TMS-evoked potentials.

Also other changes in the state of the brain cause modulation in the TMS–EEG deflections. Kähkönen et al. (2003) demonstrated with TMS–EEG that alcohol consumption reduces excitability in the prefrontal cortex. Nikulin et al. (2003) showed that voluntary preparation for movement modifies TMS-evoked EEG responses when the M1 is stimulated. Recently, it was demonstrated that the effects of TMS on the EEG-recorded event-related potentials (ERPs) remote to the primary stimulation site are also state-dependent; Morishima et al. (2008) gave subjects two kinds of tasks which changed TMS modulation in the ERPs.

In addition to measuring the changes in the brain state, TMS can be itself used to modulate the state. The effects of TMS modulation can then be evaluated using additional single-pulse TMS and EEG. A common way is to first target repetitive TMS (rTMS) to the desired brain region followed by a subsequent single-pulse stimulus. Van Der Werf and Paus (2006) showed that facilitatory rTMS at 0.6 Hz on the M1 had a significant increasing effect on the subsequent N45 deflections. Similarly, Esser et al. (2006) showed that by applying rTMS on the M1 at 5 Hz, it is possible to significantly potentiate single-pulse deflections with latencies of 15–55 ms. Another important method is the so-called paired-pulse protocol, which will be elaborated further in the next section.

2.3 Paired-pulse measurements

The paired-pulse method is a technique where the subject is given two pulses; first the conditioning pulse is used to set the cortex into a certain state and this state is studied with a subsequent test pulse. Paired-pulse methods can be divided into interhemispheric (*e.g.*, Daskalakis et al., 2002; Mochizuki et al., 2004; Koch et al.,

2009), intrahemispheric (*e.g.*, Civardi et al., 2001; Karabanov et al., 2013), and intracortical (*e.g.*, Fitzgerald et al., 2008; Farzan et al., 2010; Ferreri et al., 2011) modulation. In interhemispheric and intrahemispheric modulation, two TMS coils are set to stimulate remote cortical areas with an appropriate inter-stimulus interval (ISI).

Intracortical modulation is technically the simplest one to conduct, because there both stimuli are given with the same coil in the same position. However, by changing the ISI (Valls-Solé et al., 1992; Claus et al., 1992; Kujirai et al., 1993; Ziemann et al., 1998) or (and) the intensity (Kujirai et al., 1993; Ilić et al., 2002) of the conditioning pulse one can have drastically different effects on the cortical excitability: facilitation, inhibition, or no measurable effect. The fact that different conditioning intensities modulate the brain state differently has been explained with the neural-population-dependent activation threshold; with low conditioning intensity, low-threshold inhibitory circuits are activated more easily whereas higher intensities activate both inhibitory and excitatory circuits (Ilić et al., 2002). Depending on the used ISI and induced effects, intracortical modulation can be further divided into three different subclasses based on the stimulation parameters: short-interval intracortical facilitation (SICF), short-interval intracortical inhibition (SICI), and long-interval intracortical inhibition (LICI).

Most often the effects of the conditioning pulse on cortical excitability have been quantified by measuring MEPs from peripheral hand muscles using EMG. If a conditioning pulse and a test pulse together generate MEPs with larger amplitudes than the test pulse alone, the conditioning pulse is assumed to facilitate cortical excitability. In the opposite case, cortical inhibition is thought to take place. (*e.g.*, Valls-Solé et al., 1992; Claus et al., 1992; Kujirai et al., 1993; Ziemann et al., 1998; Ilić et al., 2002).

In addition to EMG, also epidural recordings have been combined with paired-pulse TMS to study the origin of the MEP modulation. When TMS is targeted to the M1, epidural recordings show a series of high-frequency waves: the largest called D-wave and the descending volleys called I-waves (*e.g.*, Wassermann et al., 2008). These waves are believed to reflect the level of activation generated with the stimulation. Di Lazzaro et al. (1998) showed that a low-intensity conditioning pulse failed to generate I-waves by itself but reduced the amplitude of the I-waves I2, I3, and I4 that resulted from the test pulse indicating that SICI has a cortical origin. Di Lazzaro et al. (1999) performed a similar study for SICF and showed an increase in I2 and I3 now implying that also SICF takes place in the cortex.

Although effects of paired pulses have more commonly been studied using EMG or epidural recordings, LICI has already been studied using TMS–EEG (Fitzgerald et al., 2008, 2009; Daskalakis et al., 2008; Farzan et al., 2008, 2010). The results showed that the mean signal energy[2] was decreased in a channel close to the stimulation site due to an inhibiting conditioning pulse similarly as the MEP amplitudes. Hence, these results indicate that it is possible to measure the cortical-state modulation also more directly, *i.e.*, using TMS–EEG, than evaluating muscle responses reflecting the

[2]See Section 3.3.5 for details.

excitation.

To the best of our knowledge, there are only a few works that have studied SICI and SICF using TMS–EEG. Ferreri et al. (2011) reported changes in several global mean-field-amplitude[3] (GMFA) deflections due to a difference in ISI. Similarly, they found that the potential distributions corresponding to these GMFA deflections had subtle variation over different stimulation conditions. Paus et al. (2001) used paired pulses with ISIs of 3 and 12 ms and were able to decrease the amplitudes of P30 and N45 but not the N100 amplitude.

In this Thesis, we decided to control the state of the brain by using short-interval intracortical modulation (SICM) because:

1. It enables both facilitation and inhibition.
2. The modulation of the brain state has a cortical origin.
3. There is a limited number of TMS–EEG studies probing SICM.
4. It is technically relatively easy to perform requiring only one coil with a fixed location and orientation.

[3]See Section 3.3.4 for details.

3 Methods

3.1 Data used to validate the effects of TMS on SV and MSS

We used 16 TMS–EEG datasets found in our database to test how well MSS and SV[4] are able to characterize TMS-elicited changes in the brain activity. The datasets had been measured from healthy subjects (six males and four females; age varied between 24 and 28 years) who gave their written consent before the experiments. The measurements had been approved by the Ethics Committee of the Hospital District of Helsinki and Uusimaa and they followed the principles of the Declaration of Helsinki.

Table 1: The measurement parameters in different datasets. Stimulation target refers to the cortical area controlling the named muscle: *abductor pollicis brevis* (APB) or *abductor digiti minimi* (ADM). In dataset 10, no hand muscle areas were found and stimulation was given to the area usually responsible for controlling the right hand. The stimulus intensities are given with respect to the resting motor threshold (RMT) intensity. When auditory noise masking was given, it was adjusted until the subject reported not hearing the click. The ISI either varied randomly between 2–3 s or among 1, 3, and 5 s.

Dataset	Stimulation target	Intensity [RMT]	Noise masking	ISI [s]	Number of stimuli	Coil type
1	APB	100%	Yes	2–3	100	monophasic
2	APB	100%	Yes	2–3	100	monophasic
3	ADM	100%	Yes	2–3	259	monophasic
4	APB	100%	Yes	2–3	113	monophasic
5	APB	110%	No	2–3	100	biphasic
6	APB	110%	No	2–3	100	biphasic
7	APB	90%	No	1, 3, or 5	376	monophasic
8	APB	90%	No	1, 3, or 5	306	monophasic
9	APB	90%	No	1, 3, or 5	326	monophasic
10	M1	<100%	No	2–3	60	monophasic
11	ADM	100%	No	2–3	89	monophasic
12	APB	100%	Yes	2–3	115	monophasic
13	ADM	100%	Yes	2–3	60	monophasic
14	ADM	100%	Yes	2–3	60	monophasic
15	ADM	100%	Yes	2–3	60	monophasic
16	APB	100%	Yes	2–3	60	monophasic

In all datasets, TMS stimuli were given with the same Nexstim eXimia system using a figure-of-eight coil with the outer loop diameter of 70 mm. The stimuli were targeted to the right-hand area at the left M1. Similarly, the TMS-compatible EEG device (Nexstim eXimia) was the same in all datasets. All the electrodes were

[4]See Section 3.3.2 for the exact definitions.

prepared so that their impedances were below 5 kΩ. Additionally, two electrodes were attached close to the eyes to record ocular artifacts. The EEG sampling frequency was 1450 Hz.

The datasets were chosen based on the overall signal quality, *i.e.*, low muscle- (Mutanen et al., 2013) and ocular-artifact (Ilmoniemi and Kičić, 2010) levels. The data acquisition and timing paradigms varied slightly across the analyzed datasets, meaning that our findings can be generalized over different measurement set-ups. The details of the measurement paradigms and exceptions are provided in Table 1[5].

To see the possible changes more clearly, only the 12 channels close to the stimulus location were used to form the signal subspace under study. Hence, only channels Fc_5, Fc_3, Fc_1, Fc_z, C_5, C_3, C_1, C_z, Cp_5, Cp_3, Cp_1, and Cp_z according to the International 10–20 system were studied.

3.2 Experimental paradigm for probing the effect of brain state on TMS–EEG responses

In order to support our findings obtained using the database, we proceeded with new measurements. We wished to test whether we could quantify the state dependence of the TMS–EEG responses. For this purpose, 6 healthy voluntary subjects (age: 23–29; 1 female, 5 male; 5 right-handed, 1 left-handed), later referred to as S1–S6, were measured. Before the experiments, the subjects gave their written consent. The experimental protocol was approved by the Ethics Committee of the Hospital District of Helsinki and Uusimaa. The measurements followed the principles of the Declaration of Helsinki.

The measurements were performed with a Nexstim eXimia system which consisted of a magnetic stimulator module, TMS-compatible EEG and EMG devices, and a tracking unit for nTMS. The sampling frequency of the EEG device was 1450 Hz, whereas EMG was sampled at 1000 Hz. All stimuli were given with Nexstim's figure-of-eight monophasic coil with the outer loop diameter of 70 mm.

Before the TMS–EEG experiment, T_1-weighted MR images had been taken of the subjects and uploaded to the eXimia system for nTMS. The EEG electrodes were prepared so that all channel impedances were less than 15 kΩ (preferably less than 5 kΩ). The reference and ground electrodes were set behind the ear and on the cheek bone, respectively, both contralateral to the stimulation hemisphere. Additionally, one electrode was fixed above the left eyebrow and one on the right side of the right eye to monitor ocular artifacts. The auditory artifact was minimized by playing white noise into the subjects' ears. The subjects were instructed to set the volume to a level that masks the coil click as well as possible but is still comfortable. The EMG electrodes were attached on the APB of the stronger hand with the belly-tendon montage.

The stimuli were given in three different sets: 100 single pulses, 100 paired pulses with a presumably inhibitory conditioning pulse, and 100 paired pulses with a presumably excitatory conditioning pulse. In the inhibitory condition, the conditioning pulse was given with 60% of the RMT and the ISI was 3 ms whereas

[5]The stimulation intensities are given in terms of RMT which is the minimum intensity needed to elicit at least 5 MEPs $\geq$50 µV in the target muscle with 10 stimuli to the M1.

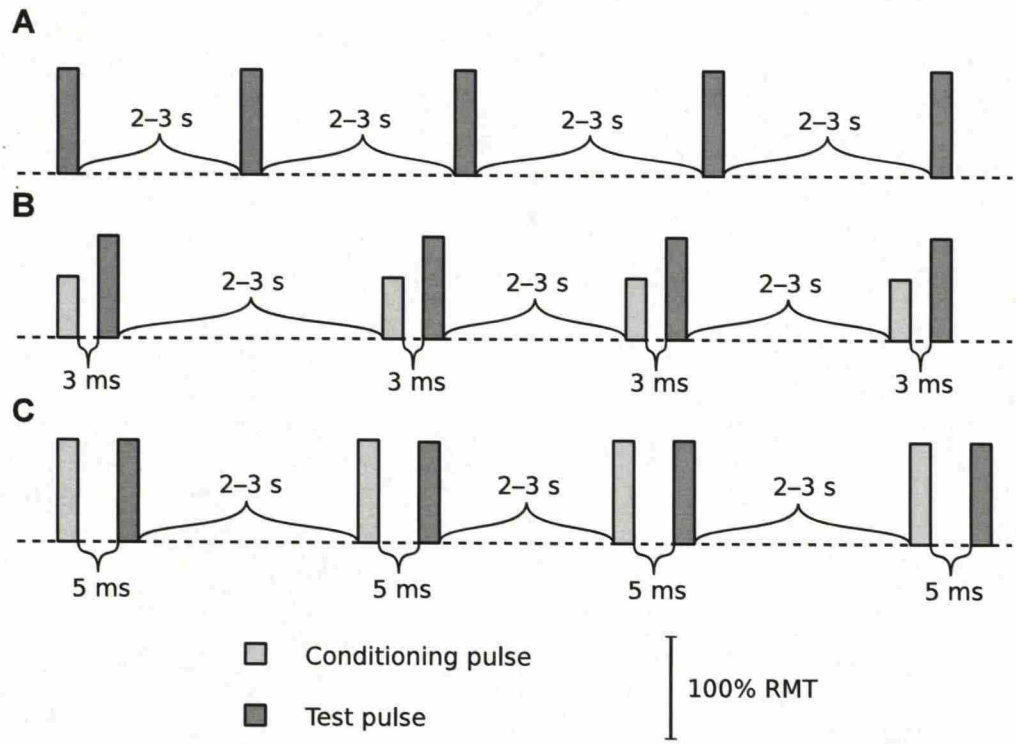

Figure 5: (A) Control condition: Single pulses with 100%-RMT intensity and random 2–3-s ISIs. (B) Inhibitory condition: Conditioning and test pulses with intensities of 60% and 100% of the RMT, respectively, with an ISI of 3 ms. (C) Facilitatory condition: Conditioning and test pulses both with 100%-RMT intensity with an ISI of 5 ms. The inter-pair interval was random 2–3 s in both paired-pulse conditions.

in the excitatory condition the conditioning pulse was 100% of the RMT with the ISI of 5 ms. In all conditions, the intensity of the test pulse was kept at 100% of the RMT. The stimulation parameters are visualized in Fig. 5. Additionally, four subjects received single-pulse sham TMS with 100%-RMT intensity so that the coil was tilted 90° with respect to the tangent of the head. Moreover, two more subjects received paired-pulse sham TMS with the facilitatory-condition parameters but with the 90° tilt. Each subject experienced the conditions in a random order.

The stimulus parameters were chosen based on the TMS–EMG literature. Our goal was to keep the test pulse the same in all conditions so that the observed changes were due to conditioning-pulse-evoked brain-state modulation. Additionally, with TMS–EEG, it is preferable to use as low stimulation intensities as possible to minimize possible muscle artifacts (Mutanen et al., 2013). On the other hand, we wanted to evoke MEPs in order to have a reliable measure of the cortical modulation in addition to EEG data. Hence, the test pulses were chosen to be 100% of RMT and the conditioning pulse were chosen based on the work by Ilić et al. (2002) (see Fig. 6).

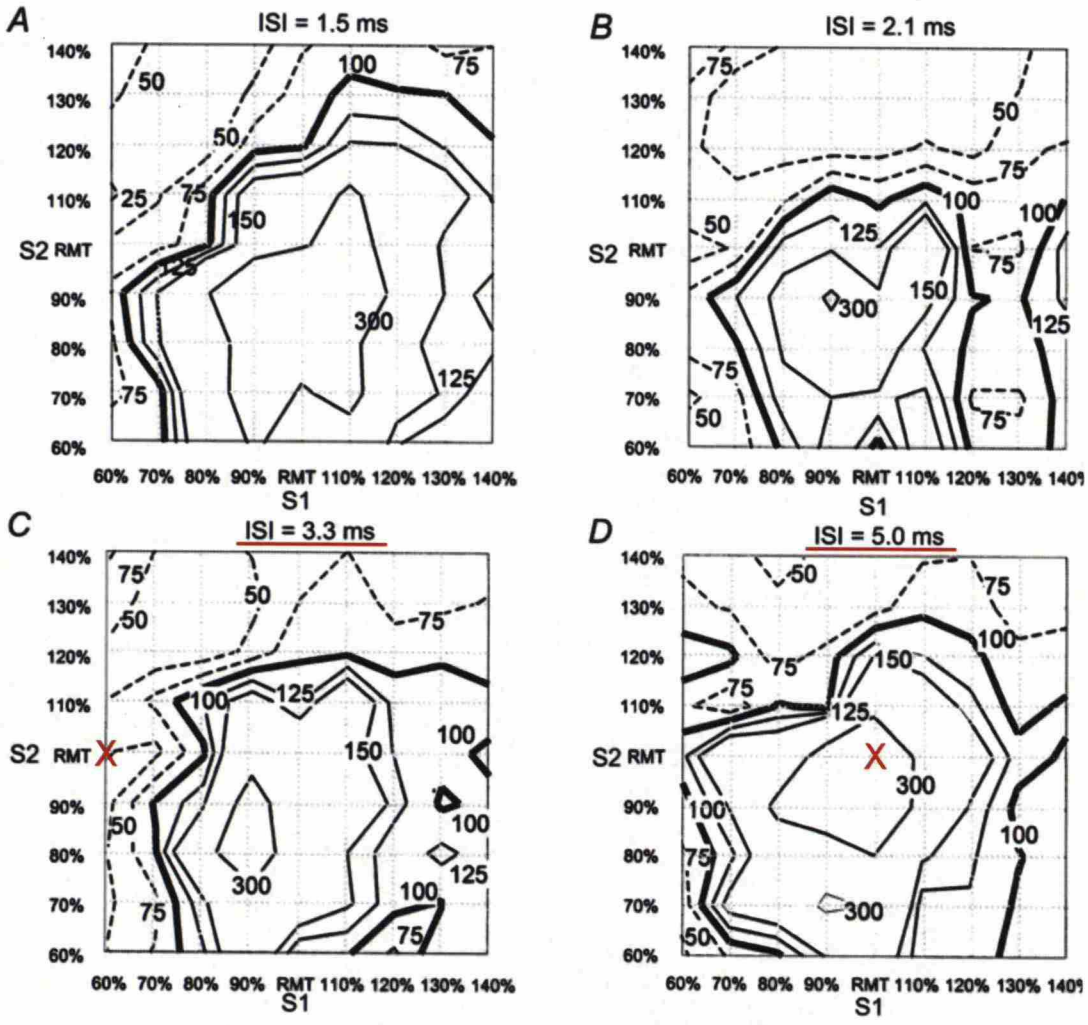

Figure 6: The effect of stimulus intensities on the MEP amplitude with different ISIs (Ilić et al., 2002). The isocontours show the differences between the paired-pulse MEP amplitudes (with successive stimuli S1 and S2) and the arithmetic sum of the MEPs evoked by single pulses S1 and S2 separately: $\mathrm{MEP}_{S1+S2}/(\mathrm{MEP}_{S1} + \mathrm{MEP}_{S2}) \times 100$. The red lines and crosses are added to highlight the parameters chosen for this Thesis in order to elicit both inhibition and facilitation.

3.3 Data analysis

3.3.1 EMG analysis

We analyzed the EMG data in a straightforward manner. Before the actual analysis, raw data were visually inspected and trials showing pre-TMS muscle tension were removed. After removing bad epochs, all the remaining trials were visually checked to identify MEPs. An EMG deflection was identified as a MEP if it started 20–24 ms after the pulse had a characteristic bipolar shape and an amplitude clearly above

the background noise level.

We mainly looked at the peak-to-peak MEP amplitudes averaged over trials when deducing whether the modulation occurred and whether it was inhibitory or facilitatory. However, also MEP likelihood $p(\text{MEP})$ was computed to estimate the probability for a MEP to occur with each stimulation parameter:

$$p(\text{MEP}) = \frac{N_{\text{MEP}}}{N_{\text{trials}}}, \tag{5}$$

where N_{MEP} was the number of observed MEPs and N_{trials} was the number of accepted trials in a particular stimulation condition.

3.3.2 Studying the effects of TMS by MSS and SV

To characterize the dynamics of the brain state during TMS by using EEG signals, we introduce two non-linear recurrence-analysis tools.

Recurrence analysis was introduced by Eckmann et al. (1987) to qualitatively analyze state-space trajectories in order to characterize different dynamic systems. Recurrence analysis describes how often and for how long a certain physical state occurs. The basic idea is simple. An appropriate threshold is first chosen. If the distance between two states is smaller than the threshold value, the state vectors are considered to represent the same state. In EEG studies, recurrence analysis has been used to study, for instance, neurological disorders (*e.g.*, Babloyantz, 1991; Pijn et al., 1997; Ouyang et al., 2008).

To provide quantitative results, several recurrence-quantification-analysis (RQA) measures, such as recurrence density, determinism, and entropy, have been introduced (Marwan et al., 2007). Strictly speaking, our measures do not fall under RQA category since we do not have any fixed threshold. Instead, we describe the obtained data by measuring average distances between state vectors. This is sometimes referred to as global recurrence (Marwan et al., 2007) or unthresholded recurrence analysis (Iwanski and Bradley, 1998; Marwan et al., 2007). However, the lack of a threshold value makes our measures more robust since one does not need to choose any arbitrary threshold. To our knowledge, RQA has not been previously applied to TMS–EEG data.

Let us now have a trajectory $\mathscr{X}$ of a system drawn in the state space, or as in our case, drawn in the EEG signal space that is a projection of the original state space. The measured trajectory consists of signal vectors at discrete time points t_l:

$$\mathscr{X} = \{\mathbf{x}(t_l) | \, t_l = t_1, t_2, \ldots, t_n\}. \tag{6}$$

The signal vector at time t_l is defined as

$$\mathbf{x}(t_l) = [x_1(t_l), x_2(t_l), \ldots, x_D(t_l)]^{\mathrm{T}}, \tag{7}$$

where D is the dimension of the signal space, defined by the number of channels, and x_j is the signal measured by channel j, defined in Eq. 4.

As the name implies, MSS describes the mean distance between state vectors belonging to two different time intervals:

$$\mathrm{MSS} \equiv \mathrm{MSS}(T_l, T_k) = \frac{1}{N_l N_k} \sum_{t_l \in T_l} \sum_{t_k \in T_k} \|\mathbf{x}(t_l) - \mathbf{x}(t_k)\|\,, \tag{8}$$

where $\| \bullet \|$ is the Euclidean distance and T_l and T_k are time intervals consisting of N_l and N_k discrete time points, respectively. Additionally, in this Thesis, we have $T_l \cap T_k = \emptyset$ and $N_l = N_k$. The purpose of MSS is to show whether there is a more dramatic average change in the state due to TMS than due to the normal fluctuations in time. Hence, MSS quantifies the immediate effect of TMS on the brain state.

On the other hand, SV measures the rate at which the state changes during a given time interval. It is anticipated that the motion of the state would be more vigorous right after the TMS pulse than before it because of the locally higher free energy, which the system tends to minimize. SV is defined as:

$$\mathrm{SV} \equiv \mathrm{SV}(T_l) = \frac{1}{N_l} \sum_{t_l \in T_l} \|\mathbf{x}(t_l) - \bar{\mathbf{x}}(T_l)\|^2\,, \tag{9}$$

where

$$\bar{\mathbf{x}}(T_l) = \frac{1}{N_l} \sum_{t_l \in T_l} \mathbf{x}(t_l)\,. \tag{10}$$

Conventionally, TMS-evoked potentials are made visible in the EEG by performing several trials and averaging the responses afterwards (*e.g.*, Komssi et al., 2002; Massimini et al., 2005; Lioumis et al., 2009). This is done to suppress the background activity that masks the TMS-evoked potentials. However, it is difficult to design a method to average both the pre- and post-TMS intervals over trials to show the TMS-evoked changes in the activity. Therefore, pre- and post-TMS activity are ideally compared at the trial level. Unfortunately, the changes due to TMS at the trial level are subtle (Mäki and Ilmoniemi, 2010). One benefit of MSS and SV is that they can be computed from trial-level data and averaged later on to highlight the TMS-elicited changes.

In the first part of this Thesis, we studied whether MSS and SV could be used to quantify TMS-caused modulations in the EEG signals. For this, we used data described in Section 3.1. Before any further data analysis, all the datasets were visually inspected. Bad EEG channels and any trials contaminated by ocular artifacts were removed. The data were also referenced with respect to the channel average and band-pass filtered at 2–80 Hz using a second-order Butterworth filter.

Both MSS and SV were calculated from unaveraged trial-level data. Each accepted trial from each dataset was divided into six different time intervals: T_1=[−200, −100], T_2=[−100, 0], T_3=[15, 115], T_4=[115, 215], T_5=[215, 315], and T_6=[315, 415], where the times are given in ms with respect to the moment of the TMS impulse (minus sign indicating time before the stimulus). Interval T_3 started 15 ms after the stimulus to ensure that the small muscle artifacts present in some datasets did not affect the results. Additionally, two time intervals, $T_{\mathrm{b}1}$=[−400, −300] and $T_{\mathrm{b}2}$=[−300, −200], were chosen for baseline scaling.

MSS was always calculated with respect to time interval T_1. Hence, for each accepted trial from each dataset, five MSS values were obtained: $\mathrm{MSS}(T_1, T_i)$, $i = 2, \ldots, 6$. MSS values were then averaged over trials for each dataset. The obtained averages were divided with the dataset-dependent average baseline value, $\mathrm{MSS}(T_{\mathrm{b1}}, T_{\mathrm{b2}})$, to suppress the differences in the datasets and to emphasize the changes due to different time intervals. The effect of time interval on MSS was studied using one-way Kruskal–Wallis ANOVA, with different subjects corresponding to different samples. After the Kruskal–Wallis test, Bonferroni-corrected *post-hoc* tests were performed to compare the grand averages of the MSS values.

SV was calculated over each time interval, providing six numerical values for each trial: $\mathrm{SV}(T_i)$, $i = 1, \ldots, 6$. The same analysis, including averaging, baseline scaling, and statistical testing described above for MSS was also applied to SV. In this case, the baseline division was done using $\mathrm{SV}(T_{\mathrm{b2}})$, again for each dataset individually.

The introduced measures can be criticized for a few reasons. First, it is not self-evident how much new information these tools are able to give about TMS–EEG data even if they would be increased after TMS. It is possible that the observed deflection would be caused by the evoked response that is added up with the natural background activity. Hence, a change in MSS or SV does not necessarily mean that the ongoing activity would be modulated. To pre-empt this argument, we performed exactly the same analysis described above for further processed data where the evoked TMS–EEG response (average over trials) was subtracted from each trial before computing MSS and SV. If the conventional assumption, that an event only adds a time-locked response to the ongoing spontaneous activity, holds, then MSS and SV should not increase in the mean-subtracted data. On the contrary, if there is still some observable increase in these measures even after mean subtraction, it implies that TMS has non-linear effects on the brain state that do not average in a conventional manner over trials.

Furthermore, one can ask how significantly the auditory and tactile responses related to the mechanical stress and click of the coil or the peripheral MEP-related somatosensory signals contribute to MSS or SV. If these responses repeat very similarly from trial to another also they are suppressed from the signal with the subtraction of the average. Of course, also these ERPs might have state-dependent characteristics making them to vary from trial to another. Anyhow, at least the muscle artifact resulting from the scalp muscle activation is probably suppressed when removing the average.

In the second part of this Thesis, we tested whether MSS and SV could be used to quantify differences in the stimulation conditions. The following analysis was performed using the data described in Section 3.2. Again, similar data preprocessing described above was done for the new data including bad-trial removal, 2–80-Hz band-pass filtering, and average referencing.

To quantify whether any of the applied stimulation parameters (ISI 3 ms, single pulse, or ISI 5 ms) had stronger effects on the brain state, MSS was computed trial-wise in each condition followed by the computation of the condition-wise average MSS. The MSS was calculated between time intervals T_1=[−110, −10] and T_2=[30, 130] using the same channels as above, except for the left-handed S4, with whom

contralaterally symmetric channels were chosen. The time intervals were chosen so that we could be certain that the muscle artifact did not contaminate the results. In addition to time intervals T_1 and T_2 we had baseline intervals T_{b1}=[−350, −250] and T_{b2}=[−210, −110] which were used to compute the average baseline MSS in each condition. Note that the baseline time intervals were separated by 40 ms as was the case with T_1 and T_2. The baseline MSS values were used to scale the actual average MSS values in each condition to make them more comparable with each other (*e.g.*, subject vigilance might change as a function of time, modulating the absolute MSS values).

Additionally, SV was computed in each condition to see whether it would change when the pre-TMS brain state would be different. This was done in two different ways: 1) similarly as MSS was studied, computing SV at each trial and averaging the obtained values over trials and 2) by computing first the average response over trials and measuring the SV using the obtained average data. From this on, we refer to the earlier as SV and to the latter as evoked SV (eSV).

When SV was studied, the same channel family specified earlier was used. To test whether the results obtained by using the database would be repeatable, SV was computed for similar time intervals: T_1=[−210, −110], T_2=[−110, 10], T_3=[30, 130], T_4=[130, 230], and T_5=[230, 330]. The small differences in the intervals are due to the fact that now some of the new data had a muscle artifact lasting for ∼30 ms. Additionally, an extra 10-ms gap was added between T_2 and T_3 since paired pulses were used. The obtained trial-level values were averaged over epochs and each condition from each subject was scaled with the condition-specific baseline value.

An eSV was computed over the time interval 30–130 ms. Since the quantified trajectory was now the average over all trials, we used the information from all the accepted channels to have as much spatial information as possible. Finally, the effect of the brain state just before the test pulse on SV and eSV was analyzed at both the subject and group levels.

3.3.3 Estimating the noise sensitivity of SV and MSS

After quantifying the effects of TMS on MSS and SV we studied how sensitive the introduced measures would be to noise. In this context, all the EEG signals generated by sources outside the brain and the brain activity not affected by TMS are considered noise, since they hide the possible TMS-elicited state shifts or increased state modulation.

We tested the effect of the noise level on the ability of the measures to distinguish between pre- and post-TMS activity by adding simulated noise to the studied database data. This can be considered a conservative estimate since the studied data are likely to already initially suffer from a considerable amount of noise.

In total, we added four types of noise: 1) stationary and uncorrelated, 2) stationary and correlated, 3) non-stationary and uncorrelated, and 4) non-stationary and correlated. Here, correlation refers to the correlation over time across different channels, whereas the stationarity refers to the variation of the noise amplitude in time.

The stationary and uncorrelated noise was simulated using MATLAB's pseudo-random number generator, drawing samples from the normal distribution with zero mean and standard deviation of 1 µV. The noise was added to each trial of each dataset separately so that contaminated data $\hat{\mathbf{X}}$ were obtained:

$$\hat{\mathbf{X}} = \mathbf{X} + \alpha\mathbf{N}, \tag{11}$$

where $\mathbf{X}$ is the original data matrix of a trial with D row vectors corresponding to good EEG channels sampled N times, $\mathbf{N}$ is the noise matrix, and α is the noise scaling factor which was increased step-by-step so that the $\mathbf{N}$ had root-mean-square (RMS) values of $\{0, 0.1, 0.2, \ldots, 2\}$ with respect to RMS($\mathbf{X}$).

The correlation of the noise was gradually increased using the following scheme. First, the noise matrix was baseline shifted so that each row of $\mathbf{N}$ would have a positive non-zero mean. For the baseline shift we empirically chose to use the value 0.5 µV. Then singular value decomposition (SVD) was used to project noise onto orthonormal components (column vectors of $\mathbf{U}$):

$$\mathbf{N} + 0.5\,\mu\mathrm{V} = \mathbf{U}\mathbf{\Sigma}\mathbf{V}^{\mathrm{T}}, \tag{12}$$

where the columns of $\mathbf{U}$ and $\mathbf{V}$ are the left and right singular vectors, respectively, and $\mathbf{\Sigma}$ has the singular values $\sigma_1, \sigma_2, \ldots, \sigma_D$ on the diagonal in descending order.

The correlation between the rows of $\mathbf{U}\mathbf{\Sigma}\mathbf{V}^{\mathrm{T}}$ can be increased by changing $\mathbf{\Sigma}$ as follows:

$$\mathrm{diag}(\mathbf{\Sigma}_n) = \mathrm{diag}(\mathbf{\Sigma}) + \gamma \cdot \mathrm{diag}(D^n, (D-1)^n, \ldots, 1^n), \tag{13}$$

where $\gamma = 0.1 \sum_{i=1}^{D} \sigma_i / D$ and n is an order parameter. The faster the singular values $\{\sigma_i | \, i = 1, 2, \ldots, D\}$ decrease when i increases, the more there is correlation between the rows of $\mathbf{U}\mathbf{\Sigma}\mathbf{V}^{\mathrm{T}}$. If there would be only one non-zero singular value, the noise would correlate perfectly whereas with $\{\sigma_i = \text{constant} | \, i = 1, 2, \ldots, D\}$ the noise would be completely uncorrelated. Hence, by increasing the order parameter we are able to increase the correlation in $\mathbf{N}$, which can now be written as

$$\mathbf{N}_n = \mathbf{C}_n(\mathbf{U}\mathbf{\Sigma}_n\mathbf{V}^{\mathrm{T}} - \mathbf{B}_n), \tag{14}$$

where $\mathbf{B}_n$ and $\mathbf{C}_n$ are n-dependent correction matrices that force each row of $\mathbf{N}_n$ to have zero mean and RMS value of 1 µV, respectively, after the correlation addition scheme. The correlation of $\mathbf{N}_n$ vs. n can be seen in Fig. 7.

Finally, the noise was made non-stationary by using equation

$$\mathbf{N}_{n,\mu} = \mathbf{C}_n(\mathbf{U}\mathbf{\Sigma}_n\mathbf{V}^{\mathrm{T}} - \mathbf{B}_n)\mathbf{S}, \tag{15}$$

where $\mathbf{S}$ is an $N \times N$ diagonal matrix with entries

$$s_{ll} = \exp\left(-(t_l - \mu)^2 / 2\beta^2\right), \tag{16}$$

where t_l is a discrete time point in a trial, $\beta = 50$ ms, and μ is the randomly chosen moment, which determines the instant of maximum noise, varying uniformly distributed between −300 and 330 ms.

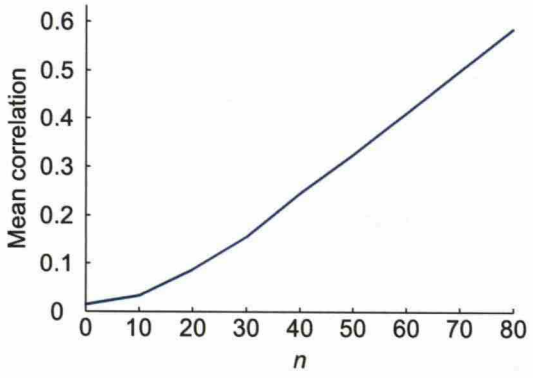

Figure 7: The mean entry in a correlation matrix computed from $\mathbf{N}_n$ as a function of the order parameter n.

3.3.4 Analyzing TMS-evoked EEG responses

Conventionally, the effects of TMS on cortical activity have been studied by applying similar TMS pulses several times and averaging the obtained EEG signals over the measured trials. This allows the study of ERPs which are assumed to recur unchanged in all trials whereas the noise, *i.e.*, the background brain activity and the noise of the measurement set-up, is leveled down by averaging. A common approach is to choose EEG channels close to the region of interest (ROI) in the brain and analyze the latencies and amplitudes of the event-related deflections in those channels. For instance, in the context of this Thesis, the researcher could expect to see some changes in these values due to different TMS parameters.

Instead of choosing ROI channels, one can compute GMFA (Lehmann and Skrandies, 1980):

$$\mathrm{GMFA}(t) = \sqrt{\frac{1}{D}\sum_{i=1}^{D}\Big(x_i(t) - \bar{x}(t)\Big)^2}, \tag{17}$$

where D is the number of channels, $x_i(t)$ is the voltage measured by channel i at time point t and $\bar{x}$ is the average over all channels. Mathematically, GMFA is the standard deviation over channels at a certain time point. Especially the moments of large amplitude in GMFA, *i.e.*, large standard deviation over channels, are considered to reflect relevant information about the event-related activity.

The apparent benefit of GMFA is that the researcher does not have to choose the EEG reference or the channels of interest since both of these degrees of freedom are determined by the definition Eq. 17. In consequence, comparisons to results in literature become more robust. Similarly as when analyzing separate channels, one can try to find differences in the amplitudes and latencies of GMFA peaks in different conditions. In the literature, GMFA is nowadays a well-established measure used to analyze TMS-evoked effects in the EEG signals (*e.g.*, Komssi et al., 2004; Massimini et al., 2005; Komssi et al., 2007; Ferreri et al., 2011). Hence, it is a good tool to benchmark the measures introduced in this Thesis.

Some of the measured datasets had clear muscle-artifact contamination during the first few tens of milliseconds. Since the ISI was very short, either 3 or 5 ms, it is quite likely that the possible differences between different conditions are found in the early latency deflections. Thus, we needed to use an offline artifact-removal method. We chose to use a signal space projection (SSP) (Uusitalo and Ilmoniemi, 1997) method tailored to remove TMS–EEG muscle artifacts (Mäki and Ilmoniemi, 2011) because it is computationally very efficient. Furthermore, it requires no heuristic classification of components into artifactual or brain-signal types, which is often the case for instance with independent component analysis.

The algorithm is simple. Since the early artifacts involve a much broader frequency band than the brain activity (Mäki, 2011), it is possible to exclude all the brain activity from the signals by high-pass filtering the data:

$$H\big(\mathbf{x}(t)\big) = H\big(\mathbf{b}(t) + \mathbf{a}(t)\big) = H\big(\mathbf{a}(t)\big)\,, \tag{18}$$

where $H(\,\bullet\,)$ is the high-pass filter in the temporal dimension, $\mathbf{x}(t)$ is the measured signal vector at time point t, and $\mathbf{b}$ and $\mathbf{a}$ are the brain and artifact components of the signal vector, respectively.

The high-pass-filtered data can be used to estimate the signal sub-space sufficient to represent most of the artifactual variance. A matrix $\mathbf{A}$, which has the $\mathbf{a}(t)$ vectors as columns, can be written using SVD as

$$\mathbf{A} = \mathbf{U}\mathbf{\Sigma}\mathbf{V}^{\mathrm{T}}\,. \tag{19}$$

The column vectors, $\mathbf{u}_1, \mathbf{u}_2, \ldots, \mathbf{u}_D$, of $\mathbf{U}$ form an orthonormal basis for the whole signal space so that the singular value σ_l describes the variance of artifactual signal in the $\mathbf{u}_l$ direction. Hence, one can remove most of the artifactual signal by projecting out the signal subspace spanned by vectors $\mathbf{u}_1, \mathbf{u}_2, \ldots, \mathbf{u}_R$, where R is the number of dimensions to be removed.

Thus, we will have an artifact-removal operator $\mathbf{P}_R$, which we can use to clean our original data matrix $\mathbf{X}$:

$$\tilde{\mathbf{X}} = \mathbf{P}_R\mathbf{X}\,, \tag{20}$$

where $\mathbf{X}$ is the data matrix having $\mathbf{x}(t)$ vectors as columns, $\tilde{\mathbf{X}}$ is the cleaned data matrix, and $\mathbf{P}_R$ can be determined as follows:

$$\mathbf{P}_R = \mathbf{I} - [\mathbf{u}_1, \mathbf{u}_2, \ldots, \mathbf{u}_R][\mathbf{u}_1, \mathbf{u}_2, \ldots, \mathbf{u}_R]^{\mathrm{T}}\,. \tag{21}$$

The successfulness of the algorithm depends on the orientation of the brain components. The less variation there is in the brain activity of interest in the direction of the artifact signal the less neural signal is removed. Since we are studying the motor cortex, it is reasonable to expect that the interesting brain activity and muscle artifacts differ in their overall direction at least to some extent.

3.3.5 Energy measure of modulation

This far, LICI has been studied much more extensively using TMS–EEG than SICI or SICF. When analyzing EEG signals, the level of inhibition has been quantified

with a simple measure (Fitzgerald et al., 2008, 2009; Daskalakis et al., 2008; Farzan et al., 2008, 2010):

$$\left(1 - \frac{\tilde{A}_i}{A_i}\right) \times 100\%, \tag{22}$$

where

$$A_i = \int_T |x_i(t)| dt, \tag{23}$$

T is the studied time interval, $x_i(t)$ is the voltage measured by the channel of interest i at time point t, and $\tilde{A}_i$ refers to the same value after inhibition. In this Thesis, we make slight changes to this quantitative tool and call it as the energy measure of modulation[6] (EMM).

Because the measure was originally introduced to quantify the degree of inhibition, the sign is positive when the area under the studied signal is smaller after modulation. However, in this work we are interested in brain-state modulation in general. Hence, by changing signs in Eq. 22, a positive value means facilitation whereas a negative value indicates inhibition. Second, instead of just choosing one channel, we are looking at the average over channels lying over a ROI. Thus, we quantify the level of modulation with the following formula:

$$\eta = \left(\frac{\tilde{A} - A}{A}\right) \times 100\%, \tag{24}$$

where

$$A = \int_T \left| \left(\frac{1}{N_{\text{ROI}}} \sum_{i \in \text{ROI}} x_i(t) \right) \right| dt, \tag{25}$$

and N_{ROI} is the number of channels belonging to the ROI.

In the works by Fitzgerald et al. (2008, 2009); Daskalakis et al. (2008); Farzan et al. (2008, 2010), EMM was computed over a time interval starting from the first artifact-free moment at 30–50 ms. Similarly, all our datasets had artifact-free data starting from 30 ms or earlier. The ending of the time interval was chosen to be at 130 ms, which was used in studies by Fitzgerald et al. (2008); Daskalakis et al. (2008); Farzan et al. (2010), enabling reliable and direct comparison to literature. Since we had two modulation conditions, ISI 3 ms and ISI 5 ms, and one control condition with single pulses, we got two EMM values for each subject. These values were then compared at both the subject and group levels.

[6]Strictly speaking the energy of a signal is defined as $E_s = \int_T |x(t)|^2 dt$.

4 Results

4.1 MSS and SV are transiently increased by TMS

TMS seemed to have the anticipated effects: Both SV and MSS were increased (Fig. 8 and Fig. 9). Fig. 8 A represents the dataset-level data showing that 15/16 datasets had an increase in SV due to TMS. Hence, also Kruskal–Wallis showed that the time interval had a significant effect on SV ($p < 0.001$). Furthermore, *post-hoc* tests revealed a significant increase in SV during time interval T_3 compared to SVs measured at the other time intervals (Fig. 8 B). At the group level, SV(T_3) was about 50% higher than the baseline value, SV(T_{b2}).

To show that the observed changes included also additional information to evoked responses, similar analysis was performed over the data which had the trial-average subtracted. Kruskal–Wallis showed the same significance level for the effect of time interval ($p < 0.001$). Also the grand-average results were qualitatively very similar (Fig. 8 D). However, Fig. 8 C, which visualizes the dataset-level results after mean subtraction, shows increased dataset-level variation, which resulted in more ambiguous results. The significance levels of the *post-hoc* tests had moderately increased (Fig. 8 D). Nonetheless, the grand average still showed ~15–20% increase in SV during T_3 compared to the other time intervals. Hence, the non-evoked parts of the post-TMS brain signal also contributed to the increased SV value.

Also in the case of MSS, a clear transiently increasing trend can be seen in most of the datasets right after TMS (Fig. 9 A), resulting in an overall significant effect ($p < 0.001$) of the time interval. Furthermore, the *post-hoc* tests showed that the MSS right after the stimulus was significantly increased when compared to MSS(T_1, T_2), MSS(T_1, T_5), and MSS(T_1, T_6) (Fig. 9 B). With grand-average MSS(T_1, T_3) and MSS(T_1, T_4), an increase of 4–12% was observed when compared to the baseline value, MSS(T_{b1}, T_{b2}).

With MSS, the major difference between the results obtained from the analysis of the original and the mean-subtracted data can be seen in Fig. 9 A and C. After mean subtraction, there is still a subtle increasing trend subsequent to TMS but less pronounced (the time interval still had an overall significant effect with $p < 0.001$). Fig. 9 D shows, that although the *post-hoc* tests could not show anymore such clear effects, the grand-average MSS(T_1, T_3) was still about 4% higher than the baseline.

In general, the results were not quite as uniform at the subject level as at the group level, although 15/16 datasets showed an increase in both SV and MSS due to TMS. However, the durations of the effects differed between subjects. In most cases, the effects lasted 100–200 ms, but in a few cases the measures did not return to the baseline level. Additionally, the dataset-level changes varied significantly: In SV, the increase was 5–300% depending on the dataset, whereas in MSS the increase was 5–30%.

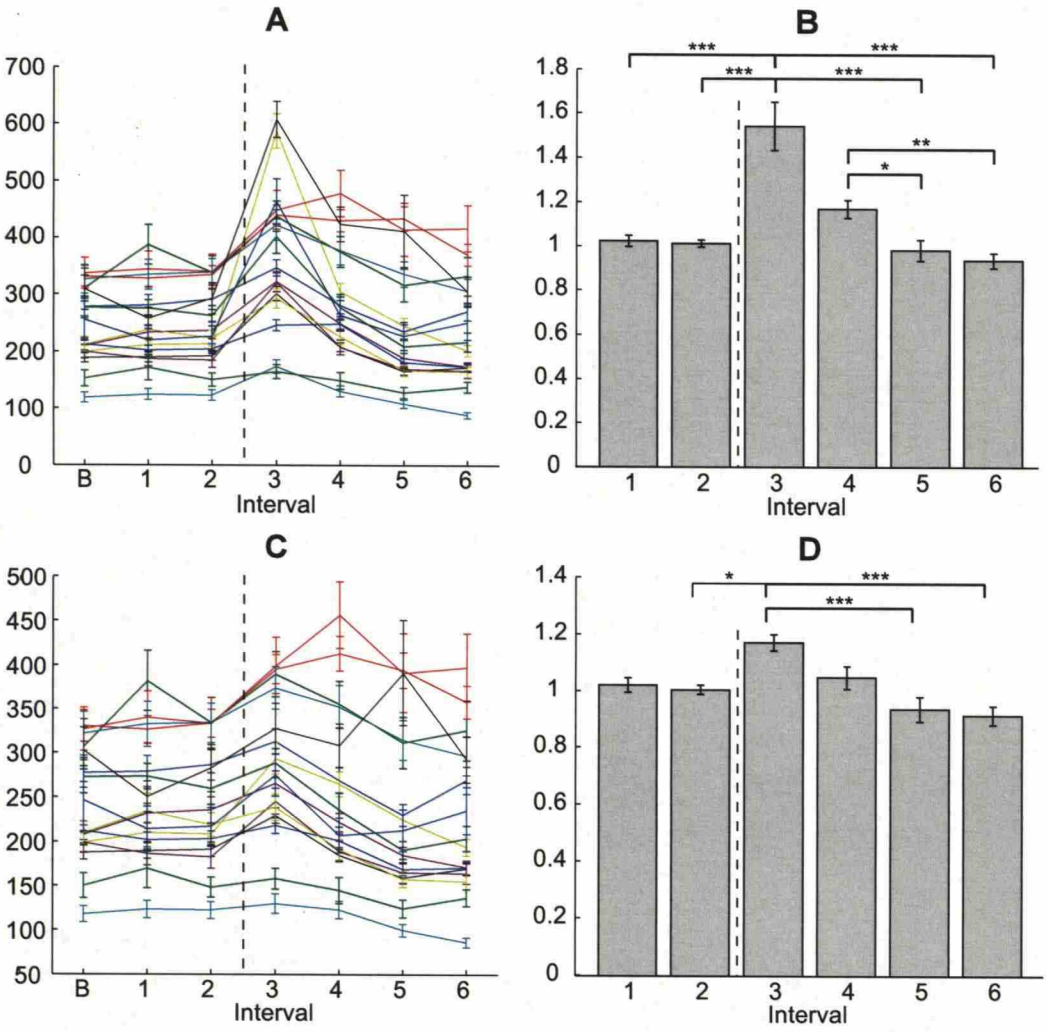

Figure 8: The effect of TMS on SV. Horizontal axes show the time interval, where B, 1, 2, 3, 4, 5, and 6 refer to time intervals (in ms) $[-300, -200]$, $[-200, -100]$, $[-100, 0]$, $[15, 115]$, $[115, 215]$, $[215, 315]$, and $[315, 415]$, respectively. The dashed lines show the moment of TMS and the asterisks indicate statistically significant differences after Bonferroni-corrected *post-hoc* tests (* $p < 0.05$, ** $p < 0.01$, *** $p < 0.001$). (A): SV averaged over trials as a function of time in all the studied datasets computed from the trial-level data. Error bars show $\pm$standard errors of the mean (SEMs) calculated over trials. Vertical axes show the absolute values of SV in μV. (B): SV at different time intervals averaged over all datasets after individual baseline scaling performed with respect to time interval B. Error bars show $\pm$SEMs calculated over different datasets. (C) and (D): Same as (A) and (B) but after the mean subtraction.

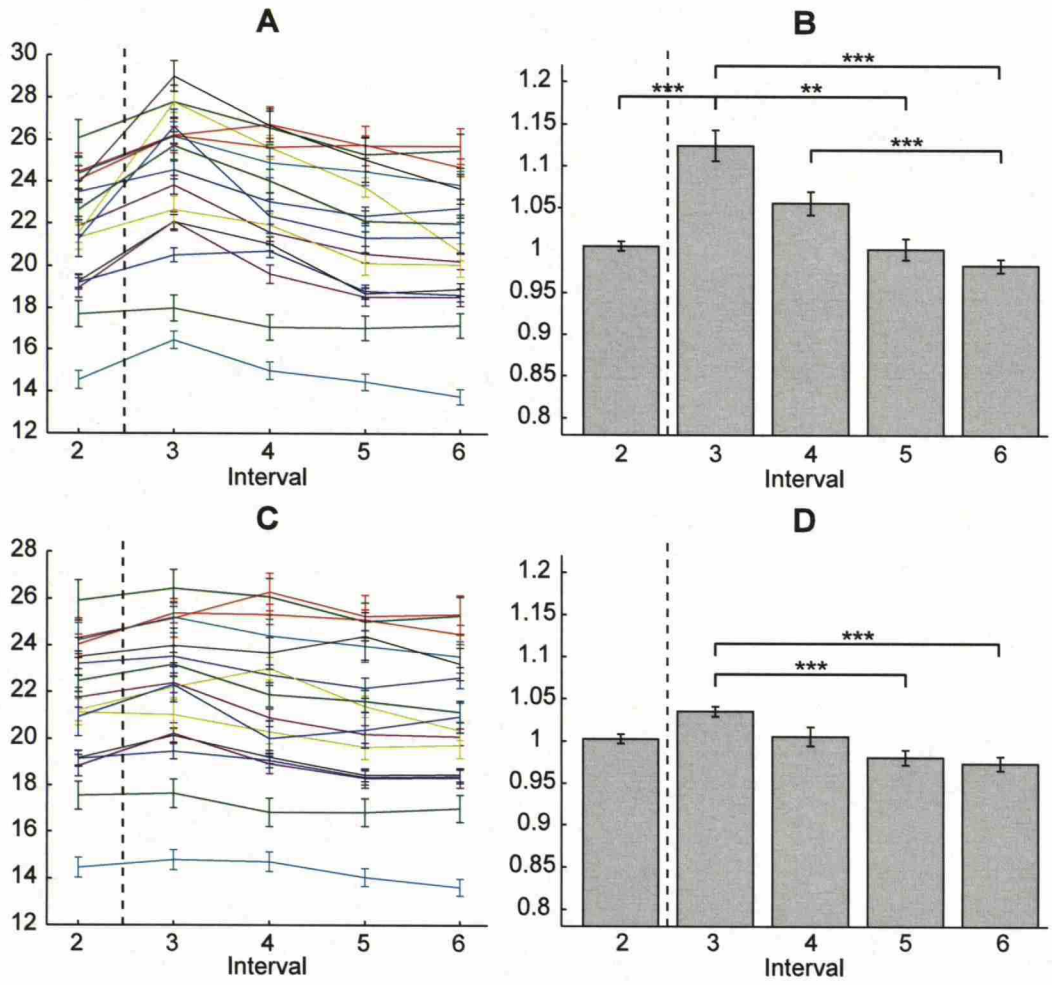

Figure 9: The effect of TMS on MSS. Horizontal axes show the time interval, where 2, 3, 4, 5, and 6 refer to time intervals (in ms) [−100, 0], [15, 115], [115, 215], [215, 315], and [315, 415], respectively. In all time intervals, the MSS has been computed with respect to $T_1 = [-200, -100]$. The dashed lines show the moment of TMS and the asterisks indicate statistically significant differences after Bonferroni-cerrected *post-hoc* tests (* $p < 0.05$, ** $p < 0.01$, *** $p < 0.001$). (A): MSS averaged over trials as a function of time in all the studied datasets computed from the trial-level data. Error bars show ±SEMs calculated over trials. Vertical axes show the absolute values of MSS in μV. (B): MSS at different time intervals averaged over all datasets after individual baseline scaling. Hence, the vertical axis shows the value of MSS with respect to the baseline value. Error bars show ±SEMs calculated over different datasets. (C) and (D): Same as (A) and (B) but after the mean subtraction.

4.2 MSS and SV seem relatively tolerant to noise

Since the effects of TMS on MSS and SV were mainly studied at the group level, also the effects of the added noise were observed at the group level. Thus, we mainly analyzed how the grand-average differences between MSS(T_1, T_2) and MSS(T_1, T_3), or SV(T_1) and SV(T_2) changed as a function of added noise. Additionally, we observed how the grand-average difference between the particular time intervals compares with the sum of the group-level standard deviations of MSS(T_1, T_2) and MSS(T_1, T_3), or SV(T_1) and SV(T_2). In general, neither MSS nor SV was very sensitive to the added noise. The main findings are presented in Figs. 10 and 11.

From the two quantitative tools, MSS was found to be less resistant to noise contamination. When stationary and uncorrelated noise was added, the grand-average difference of the pre- and post-TMS values was below the standard deviation sum at noise level higher than 1.25 RMS($\mathbf{X}$) (Fig. 10 A). However, when we increased the correlation in the simulated noise, the grand-average difference decreased much less steeply as a function of noise level (Fig. 10 B). The most severe type of noise when using MSS was clearly non-stationary uncorrelated noise. Although the grand-average difference decreased slowly, variation of MSS during all time intervals increased rapidly (Fig. 10 C). However, correlated non-stationary noise contaminated the results slightly less (Fig. 10 D).

The results show that SV was especially tolerant to stationary noise (Figs. 11 A and B). When adding uncorrelated noise to the datasets, even at noise level of 1 RMS($\mathbf{X}$) the difference of grand-average SV(T_1) and SV(T_2) was still almost 20%. Furthermore, the summed standard deviations did not exceed SV(T_2)−SV(T_1) until the noise level was up to 2 RMS($\mathbf{X}$). As was the case with MSS, adding correlation decreased the effects of noise to the results. Also SV was most sensitive to non-stationary noise. At noise level of ~1 RMS($\mathbf{X}$) and higher, the sum of standard deviations exceeded the observed difference of pre- and post-TMS SVs (Fig. 11 C). The main difference with non-stationary noise between MSS and SV was that the value of SV(T_2), in terms of the baseline level, decreased much faster as a function of noise level. In the non-stationary-noise condition, the correlation of the noise had to be increased significantly before the contamination started to decline (Fig. 11 D).

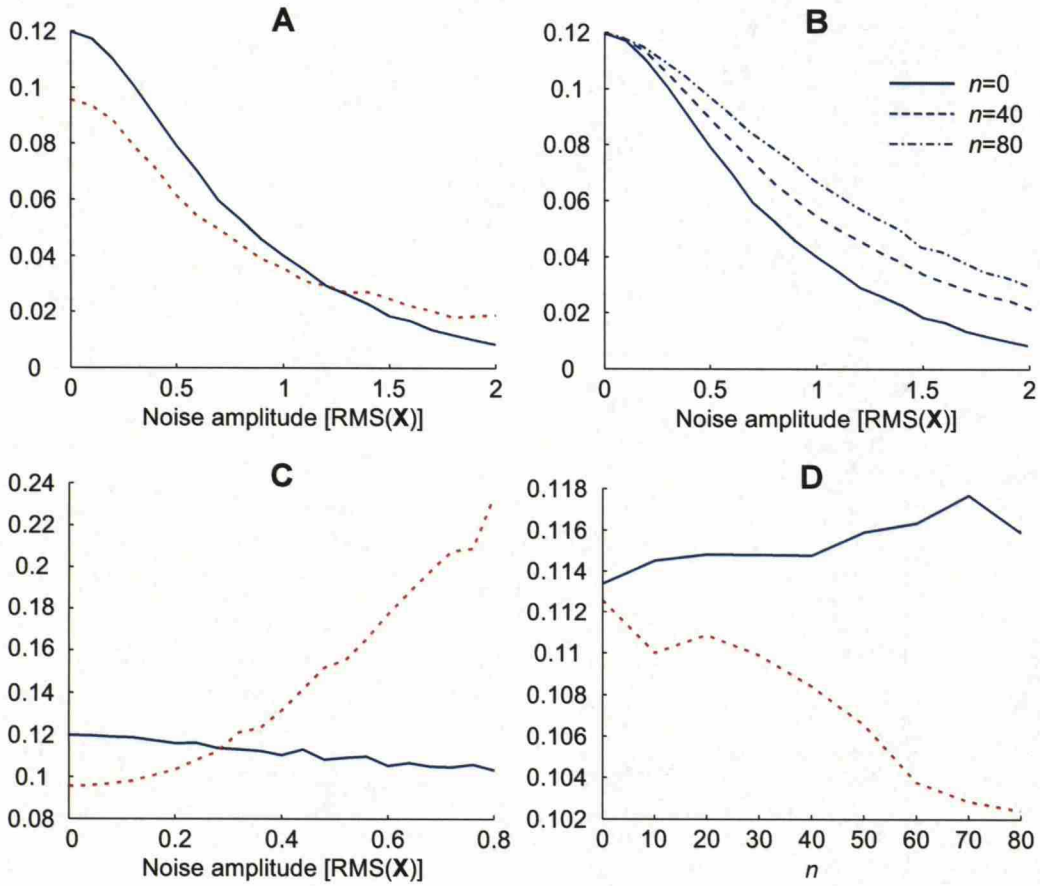

Figure 10: The effect of added noise on MSS analysis. (A): The effect of stationary uncorrelated noise on grand-average-MSS results. The solid blue line shows the difference of grand-average MSS(T_1, T_2) and MSS(T_1, T_3) values while the dashed red line shows the sum of the group-level standard deviations of MSS(T_1, T_2) and MSS(T_1, T_3) as a function of noise level. (B): The effect of stationary noise with three different correlation levels. The curves show the difference of grand-average MSS(T_1, T_2) and MSS(T_1, T_3) values. (C): Same as (A) but with non-stationary uncorrelated noise. (D): The effect of correlation level of the non-stationary noise on the difference of grand-average MSS(T_1, T_2) and MSS(T_1, T_3) values (solid blue line) and the sum of the group-level standard deviations of MSS(T_1, T_2) and MSS(T_1, T_3) (dashed red line) with the noise level of 0.30 RMS(**X**).

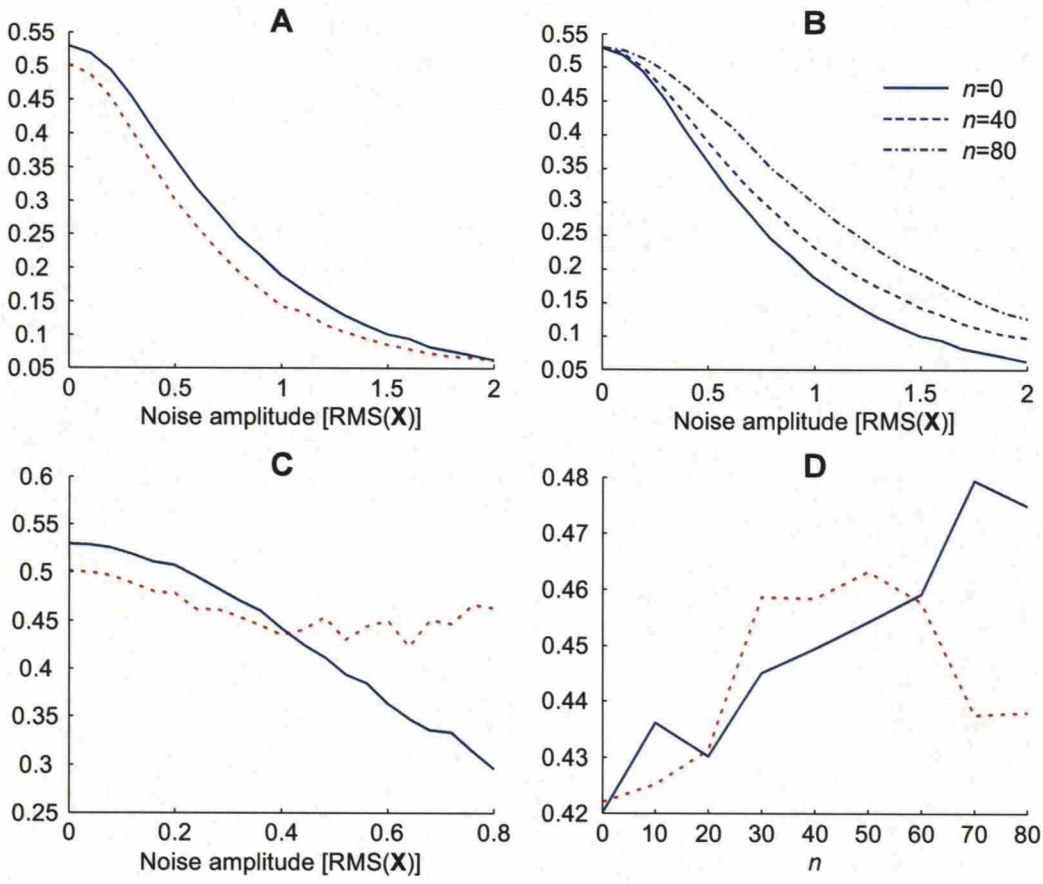

Figure 11: The effect of added noise on SV analysis. (A): The effect of stationary uncorrelated noise on grand-average-SV results. The solid blue line shows the difference of grand-average SV(T_2) and SV(T_3) values while the dashed red line shows the sum of the group-level standard deviations of SV(T_2) and SV(T_3) as a function of noise level. (B): The effect of stationary noise with several correlation levels. The curves show the difference of grand-average SV(T_2) and SV(T_3) values. (C): Same as (A) but with non-stationary uncorrelated noise. (D): The effect of correlation level of the non-stationary noise on the difference of grand-average SV(T_2) and SV(T_3) values (solid blue line) and the sum of the group-level standard deviations of SV(T_2) and SV(T_3) (dashed red line) with the noise level of 0.40 RMS($\mathbf{X}$).

4.3 Conditioning pulses modulate MEPs

The results obtained from the measurements performed for this Thesis showed clearly that it is possible to modulate the MEP amplitude and likelihood by giving paired pulses with different parameters.

Especially paired-pulse stimulation with the ISI of 5 ms and 100%-RMT conditioning intensity showed repeatable results over all six subjects. As expected, based on an earlier study by Ilić et al. (2002), the particular stimulation parameters resulted in the facilitation of MEPs. Both the MEP amplitude and likelihood were increased in all the subjects (see Fig. 12). While with single pulses with 100%-RMT intensity the mean MEP amplitude over trials varied over subjects from 34 to 386 µV, with the ISI of 5 ms the mean MEP amplitudes were 51–2077 µV, meaning a subject-level increase of 65–438%. In consequence, the grand-average-MEP amplitude was increased 237%, from 221 to 747 µV. Also the MEP likelihood was increased, on average 37 percentage points, in all subjects.

Also with the 3-ms ISI, it was possible to modulate MEPs compared to single pulses. However, the subject-level results were much more ambiguous. With S2 and S6 MEP amplitude and MEP likelihood were inhibited, whereas S1 and S3 showed small facilitation. With S4 and S5, the changes in amplitude and likelihood were in opposite directions. The grand-average-MEP amplitude was decreased 9 percent, from 221 to 201 µV.

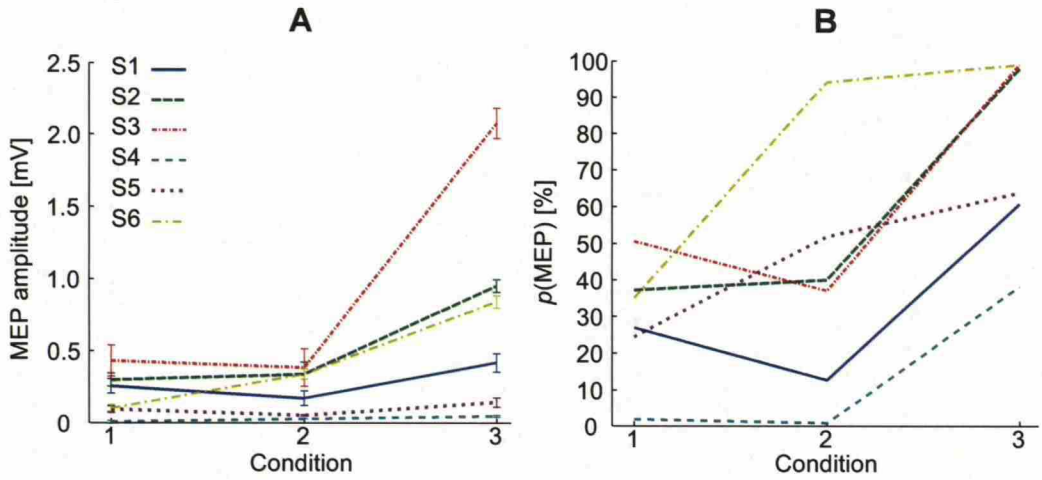

Figure 12: The effect of different stimulus parameters on MEPs. The conditions 1, 2, and 3 on the horizontal axes refer to the ISI of 3 ms, single pulses, and the ISI of 5 ms, respectively. (A) MEP amplitude as a function of different stimulus parameters measured from each subject. The error bars show the SEMs calculated over trials. (B) MEP likelihood as a function of different stimulus parameters measured from each subject.

To control whether SICM could be visible in EEG using an already established EEG measure, we computed EMM and compared it to the MEP results. The

EMM values are presented with the corresponding MEP results in Fig. 13. At the group level, the EMG and EEG results correspond with each other relatively well. All subjects show facilitation in the 5-ms-ISI condition with respect to the MEP amplitude and the EMM. On the contrary, the grand-average-MEP amplitude and EMM showed different type of modulation in the 3-ms-ISI condition, although both values were close to zero.

However, at the subject level, EMM did not seem to produce perfectly robust results. For instance, in the 5-ms-ISI condition, S3 showed huge MEP facilitation, whereas the EMM was only slightly positive. On the other hand, S5 seemed to have significant facilitation based on EMM, although the MEP amplitude was only moderately increased.

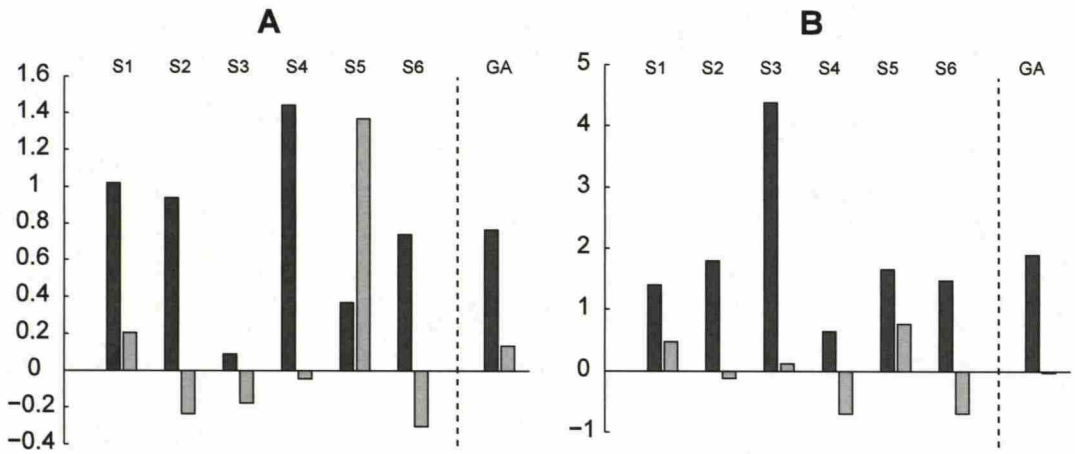

Figure 13: Comparing EEG- and EMG-based brain-state modulation measures. (A) EMM measured from each subject from the averaged EEG response. The dark bars show EMM in the facilitatory condition, whereas the light bars show the EMM in the inhibitory condition. The bars under the sign GA show the grand average over the subjects. (B) Modulation of MEPs at the subject level. The darker bars show the percentile change from the average MEP amplitude in single-pulse condition to the average MEP amplitude in the 5-ms-ISI condition and the lighter bars show the percentile change in MEP amplitudes when going from single-pulse condition to the 3-ms-ISI condition. GA refers to the grand average of the MEP modulation.

4.4 Grand-average GMFA shows increased TMS-evoked deflections in the facilitatory condition

The conventional EEG analysis was done by investigating the amplitudes and latencies of GMFA peaks. To remove muscle artifacts from the studied signals before computing GMFA, we projected out 4 dimensions from the signal spaces measured from S1, S2, S5, and S6 and 10 dimensions from the signal space of S3. For S4 data, no artifact removal was required. At the group level, the results clearly show that in the facilitatory-condition the GMFA was larger for the time interval 0–230 ms following the stimulus, whereas the inhibitory and the control conditions resemble each other much more (see Fig. 14).

Especially P30 and N100 showed increased amplitude in the 5-ms-ISI condition compared to the other two conditions. Additionally, the P60 peak was clearly much more pronounced in the facilitatory condition when compared to the single-pulse condition, but not so significantly when compared to the inhibitory condition. Also N45 was slightly potentiated in the facilitatory condition, although the difference was not that significant when compared to the SEM values.

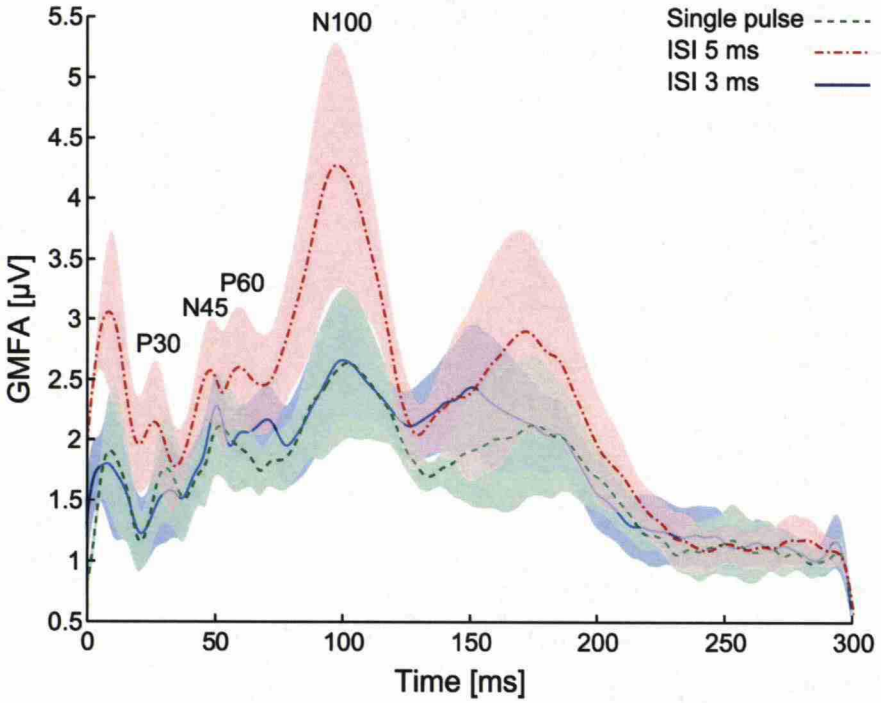

Figure 14: Grand-average-GMFA values measured in different conditions as a function of time. The shaded areas show the SEMs over subjects at each time point. The symbols P30, P45, P60, and N100 indicate several deflections of the curves. The first letter tells the polarity of the deflection in the raw data and the number the approximate latency with respect to the moment of TMS. In GMFA, the polarity of the deflection is not visible.

However, the clearest difference between the facilitatory condition and the two other conditions was around 10 ms. In this Thesis, we later refer to this deflection as P10. Responses observed this early are often left out from the analysis as they co-occur with muscle artifacts. In the obtained grand-average GMFA, the facilitated P10 amplitude showed almost two-fold increase in comparison to other conditions.

In addition to amplitude modulation, also latencies of the observed TMS-evoked deflections were changed. Especially P30 and P45 had their maximum amplitudes about 5 ms earlier in the facilitatory condition when compared to the control condition. This corresponds well with the ISI used in the facilitatory condition. In the 3-ms-ISI condition, the latencies did not differ clearly from the control condition.

Although the grand-average GMFA showed quite convincingly that the facilitatory state before the test pulse increased the overall GMFA amplitude, many details in the results were relatively variable in the subject-level GMFA curves. Only the amplitudes of P10 and P30 were increased in all the subjects due to facilitation. Other peaks showed more variation in their amplitude in different conditions. In fact, some peaks were even difficult to recognize from the subject-level data. Especially, it was difficult to distinguish between N45 and P60. Even the latency changes mentioned above were not apparent in all the subjects. The variation can be clearly seen as large shaded SEM areas surrounding the obtained grand-average curves (Fig. 14).

S3–S6 received additionally single-pulse sham stimulation. In all the subjects, the sham stimulation resulted in clearly lower amplitude GMFA. Furthermore, S4 was the only subject whose sham GMFA showed any recognizable response at ~100 ms, possibly reflecting the auditory response. Furthermore, stimulating S5 and S6 with paired-pulse sham did not produce any evoked responses notably different when compared to the single-pulse sham condition.

4.5 The measured data imply a subtle increase in MSS due to facilitation

We tested whether the paired pulses would induce a different MSS when compared to single-pulse stimulation. The results can be seen in Fig. 16. At the subject level, 5/6 subjects showed increased MSS in the facilitatory condition when compared to the single-pulse condition.

When the MSS obtained in the inhibitory condition was compared to the single-pulse MSS, the results varied more. However, when the subject-level trends of MSS were compared to those of MEP amplitude and MEP likelihood, the results seemed rather consistent.

The grand-average-MSS values showed that paired pulses with the ISI of 5 ms had elicited a larger state shift than single pulses. However, the difference between the 3-ms-ISI and single-pulse MSS values was clearly within the error limits. Overall, the grand-average values corresponded well with the MEP results (see Fig. 12 B).

The results obtained using the database were confirmed. In all subjects in all conditions, the TMS-elicited MSS was larger than the baseline MSS between two time intervals separated by a time gap identical to that separating pre- and post-TMS

time intervals. In consequence, also the post-TMS grand-average MSS was over one in all conditions, being clearly of the same order of magnitude as the grand-average result computed using our database.

Sham stimulation did not evoke any increase in MSS compared to the baseline value in any of the subjects. Furthermore, when the paired-pulse sham stimulation with the ISI of 5 ms and 100%-RMT-intensity pulses was delivered to S5 and S6, MSS was not increased from the MSS measured with the single-pulse sham.

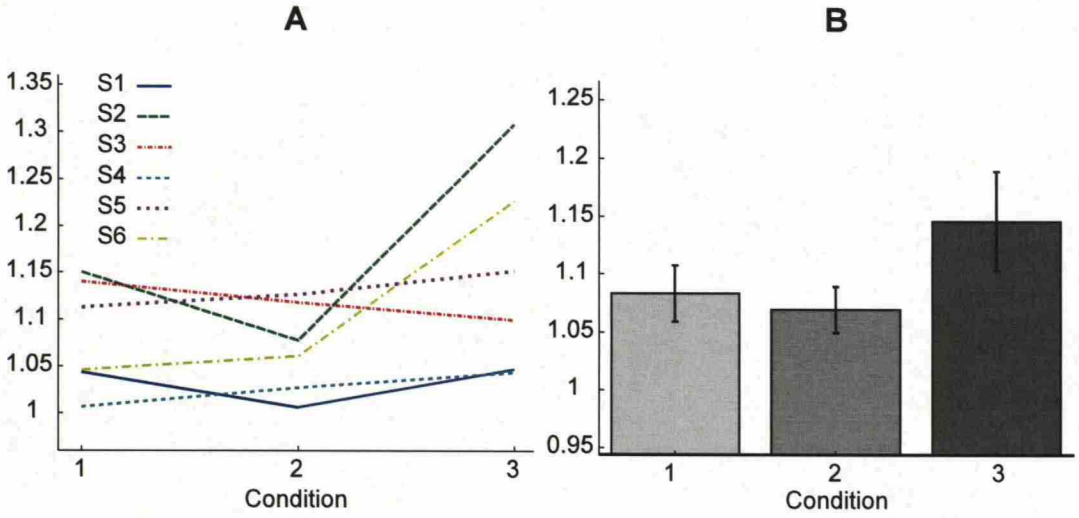

Figure 15: The effect of SICM on the TMS-elicited MSS. (A): Subject-level MSS values in all conditions. Conditions 1, 2, and 3 refer to the ISI of 3 ms, single pulse, and the ISI of 5 ms, respectively. The vertical axis gives MSS with respect to the appropriate baseline value. (B): Grand-average MSS values in all conditions (same as in A). The error bars show the SEM in each condition.

4.6 SV might correlate with the level of excitation

We repeated a very similar trial-level SV analysis on the conditioned data as we did earlier for the data gathered from the database. The main results are presented in Fig. 16. Both the subject-level and the group-level results were qualitatively very similar to those already reported in Section 4.1 and visualized in Fig. 8; SV is significantly increased immediately after the TMS pulse until the variance returns back to the baseline level.

However, when the 3-ms-ISI, 5-ms-ISI, and single-pulse conditions are compared to each other, it is evident that SV subsequent to TMS has increased much more in the facilitatory condition. The difference is visualized in Fig. 16. When all the subject-level data are plotted in gray-scale images, the facilitatory condition results in clearly lighter color during time interval 3 (30–130 ms after the pulse). The grand averages summarize the observed change. On the other hand, during the other time intervals, SV was similar in all conditions, indicating that increased state fluctuation has approximately the same duration regardless of the stimulation parameters.

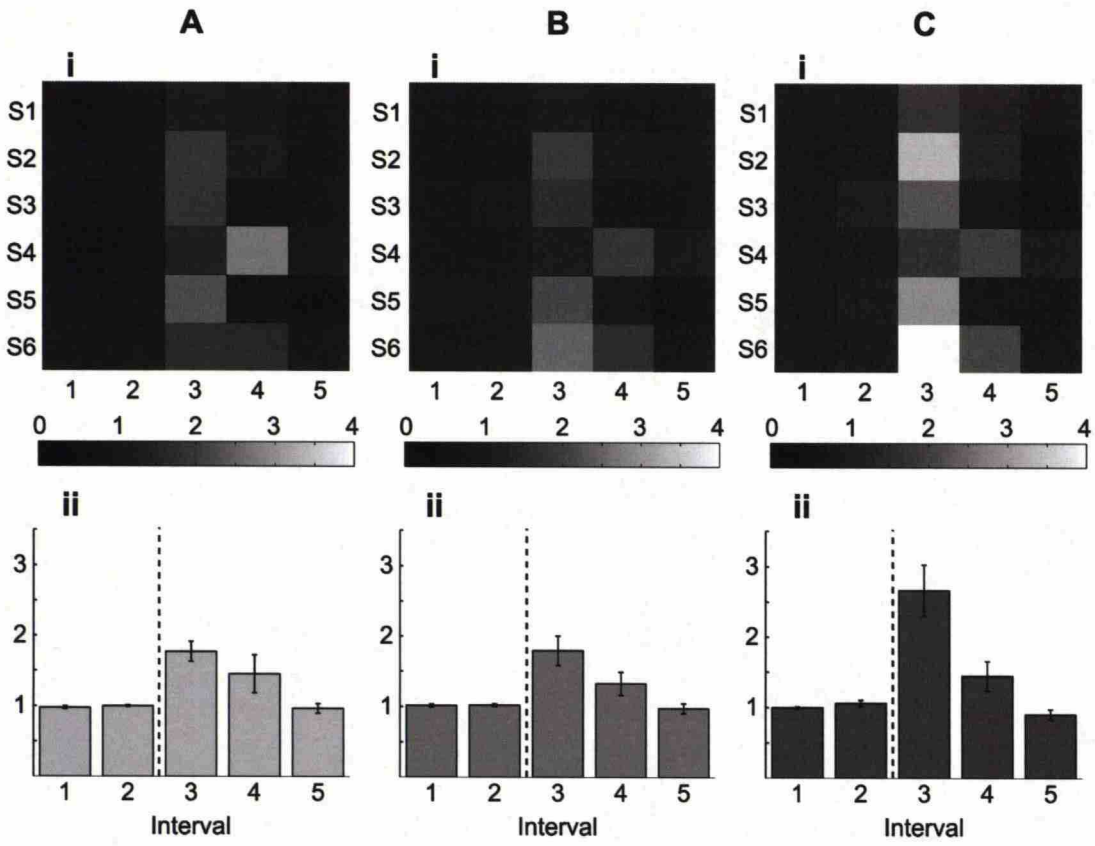

Figure 16: The effect of SICM on SV trend during TMS. (A): i) A gray-scale image showing subject-level SV as a function of time interval with the ISI of 3 ms. On the horizontal axis, the numbers 1, 2, 3, 4, 5 refer to the time intervals (ms) [−210, −110], [−110, −10], [30, 130], [130, 230], and [230, 330], whereas the vertical axis indicate the subject. The shade of the pixel illustrates the obtained SV values in terms of the subject and condition specific baseline value. The gray-value bar shows the scale for the SV values. ii) Grand-average SV as a function of time interval with the ISI of 3 ms. (B): i) Subject-level SV as a function of time interval with single pulses. ii) Grand-average SV as a function time interval with single pulses. (C): i) Subject-level SV as a function of time interval with the ISI of 5 ms. ii) Grand-average SV as a function of time interval with the ISI of 5 ms. In (A), (B), and (C), the dashed line shows the moment of TMS and the error bars show the SEMs computed over subjects.

In addition to trial-level SV computation, we analyzed the effect of condition on eSV. The results are shown in Fig. 17. At the subject level, the facilitatory condition always caused the largest eSV. Furthermore, in each subject eSV, qualitatively correlated with the average MEP amplitude in that condition. In consequence, when the eSV obtained for the ISI of 3 ms and ISI of 5 ms were scaled with the subject-wise single-pulse eSV and averaged after that over subjects, the grand-average eSV showed again clear increase in the facilitatory condition.

However, although qualitatively correct, the results were rather varying at the subject level. For four of the subjects, the difference between the eSV values in different paired-pulse conditions was quite small. This is also visible in the estimated error of the grand averages. While in the SV analysis the SEM was about 10% right after TMS, in the case of eSV the SEM was approximately 20% of the mean eSV.

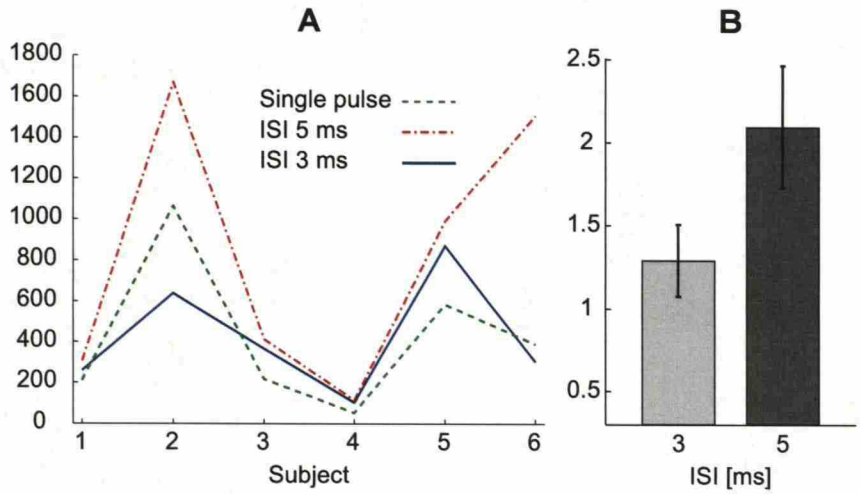

Figure 17: The effect of SICM on the eSV. (A): eSV after TMS computed from each subject in each condition. (B): Grand-average eSV in facilitatory and inhibitory conditions. The vertical axis shows eSV with respect to the grand-average eSV measured in the single-pulse condition.

5 Discussion

5.1 Indications of the SV and MSS results

Our results show that the measures introduced in this work are able to reveal differences in brain dynamics. The grand averages showed a significant increase both in SV and in MSS after TMS until they returned back to the baseline level. At the subject level, one could observe similar trends although there was inter-subject variability. Our hypothesis concerning the effects of TMS on the brain state relates to TMS in general, so in the first part of this Thesis, we use datasets with moderate differences in stimulation parameters. Indeed, we were able to see a relatively clear trend both in MSS and SV during TMS even by using varying datasets.

The increase in MSS implies that the brain activation following TMS occupies different regions in the brain state space than spontaneous activity. In the second part of this Thesis, we used three different stimulation parameters to vary the effectiveness of TMS to modulate the brain state. In the facilitatory condition, which resulted in the largest and most frequent MEPs, MSS was clearly increased. Thus, TMS was able to shift the brain state more often to a non-spontaneous brain state of evoking a MEP, increasing the trial-average MSS.

Although numerous empirical results (*e.g.*, Komssi et al., 2002, 2004, 2007; Massimini et al., 2005; Lioumis et al., 2009) lead to expect that TMS changes the primary current distribution, it is far from self-evident that the sudden shift would be measurable from trial-level EEG data, given that EEG is an extremely low-dimensional projection of the original brain state. As discussed earlier, here conventional averaging is not an option, and thus the observed shift has not been reported before. Indeed, the results show that, although the changes in MSS were statistically significant, they were still quite subtle, which is not a surprise, since the primary activation due to TMS is very focal (Hannula et al., 2005). Thus, most of the background activity is likely to stay similar even after the stimulus.

The increase in SV indicates that TMS-modulated activity differs in nature from spontaneous activity. In the grand averages, there were differences of 150% between the pre-TMS SVs and the immediate post-TMS SV, implying that TMS-modulated activity proceeds faster in the state space than the spontaneous one. Furthermore, the post-TMS fluctuation was increased further when stimulation was facilitatory, and hence the cortex was excited more. This supports the observation that MSS seemed to be larger in the facilitatory condition; shifting brain state further from the spontaneous state means increased fluctuation until the state is in some sense stabilized. In general, SV seemed to change in a state-dependent way.

To understand better what kind of brain-state behavior is visible in MSS and SV, we performed the same analysis for the database data from which we had removed the evoked response. This analysis produced qualitatively similar results as the ordinary trial-level data although the differences became less significant. Nevertheless, the results imply that MSS and SV might be able to quantify also non-linear TMS-elicited changes that are dependent on the current brain state, and thus are not visible in the averaged response. Hence, both MSS and SV might provide new information

about the effect of TMS on the brain state.

Because in the first part of this Thesis we used a database to evaluate the introduced measures, we lacked sham data. Thus, we cannot completely exclude the possibility that the increases in SV and MSS in the initial study are partially due to somatosensory or auditory responses. Indeed, white noise was delivered to the subjects' ears (Paus et al., 2001) to minimize the auditory response at ~100 ms and ~180 ms in only some of the datasets. Thus, especially the analysis of datasets 5–10 might be affected by the auditory response (Nikouline et al., 1999). However, in the second part we performed also sham stimulation to validate the effect of auditory response on SV and MSS. We observed practically no change in these measures, indicating that probably the contribution of the auditory response is quite mild.

The somatosensory response due to scalp nerve activation is likely to have a smaller contribution to the observed changes, since the studied channels located close to the stimulation site and the somatosensory responses from the scalp are seen on the contralateral hemisphere (Bennett and Jannetta, 1980; Hashimoto, 1988). However, eSV was analyzed utilizing the whole signal space. Thus, this part of the analysis might be contaminated by the tactile sensation on the scalp.

Since the stimulation intensity was in all datasets around 100% of the RMT we have to consider the possibility that the MEP-related peripheral somatosensory signal might have contributed the studied measures. Although Paus et al. (2001) and Nikulin et al. (2003) showed that the MEP-related sensations did not significantly affect the average TMS-evoked EEG responses, it would be advisable to conduct the analysis described in the present work over data measured when TMS has been delivered with sub-threshold intensity or to a non-motor area to ensure that the MSS and SV are not affected considerably by the tactile sensation of a MEP.

In the present work, we did not study the dynamic changes in solely spontaneous EEG data. However, we are convinced that the changes in MSS and SV are due to TMS (and indeed possibly due to sensory stimuli elicited by the magnetic impulse) since the increase in SV and MSS is short-lived and returns back to the baseline level.

The effects of TMS on SV and MSS seemed to last 100–200 ms. However, the length of the studied time intervals was 100 ms, limiting the temporal resolution. In principle, the temporal resolution could be improved simply by reducing the length of the time intervals. Unfortunately, this is likely to increase the relative contribution of noise in the measures. Indeed, we attempted to use shorter time intervals when studying the conditioned TMS–EEG data. However, this seemed to add random changes in the measures increasing especially subject-level variation.

Our noise simulations indicated that MSS results were faster masked under the noise-related variance. This might be due to the fact that observed TMS-elicited changes in MSS were initially much more subtle than with SV. On the other hand, the results might indicate that SV is a more robust measure, partially explaining why the results obtained from pure measurement data showed much greater increase in SV than in MSS after TMS. Not surprisingly, non-stationary noise was more severe than stationary noise, since it randomly increased MSS and SV at all time intervals hiding the effect of TMS. Hence, when using the introduced measures, the

researchers should minimize all possible extra sensory inputs that elicit random brain activity deflections in the measurement situation. A major difference in the analysis of this Thesis when compared to our publication (Mutanen et al., 2013) was the use of off-line channel average referencing. The benefits of this are visible in the noise simulation results. The correlated noise had less significant effects on the results simply because the effective RMS value of the noise was lower than the RMS value of the added noise due the average referencing.

In general, our noise simulations implied that neither MSS nor SV are highly sensitive to noise with the number of data points included to the studied time intervals in this Thesis. However, as already pointed out, shortening the length of the time interval increases the contribution of noise in the measures. For instance, if the studied time interval is halved when computing MSS the contribution of noise is doubled in the final estimate[7]. Based on Fig. 10 we can assume that an increase of noise contribution of this significance could be very harmful for the measures.

In addition to decreasing the temporal resolution, the introduced measures could be improved by developing the computation methods. In this thesis, the SV and MSS were computed in the signal space. Since the lead fields of the EEG channels are not orthogonal, we needed to orthonormalize the data using SVD. However, the orthonormalization could also be performed by projecting the measured signal vectors into computed source space components (*e.g.* by using minimum-norm estimate introduced by Hämäläinen and Ilmoniemi (1994)). The benefit of the source space analysis would be that SV and MSS would produce more direct information about the changes in the actual primary current distribution, provided that the model used to compute the source space is accurate enough.

The changes in SV and MSS, in a broad sense, can be explained with the second law of thermodynamics. Although there is a substantial physiological system constantly providing energy and information to the brain, we can approximately consider the brain as an isolated system for the short period of time (~300–400 ms) that we measure it after the impulse. The spontaneous state before the TMS impulse lies relatively low in the free-energy landscape. The large impulse forces the brain state to a new state that normally has a lower probability meaning increased free energy. The observed activation following the impulse is partially due to the brain settling itself again to a lower energy level. Similar ideas have also been presented earlier (*e.g.*, Hopfield, 1982; Friston et al., 2006; Friston, 2010), although the earlier article discusses the free energy of an artificial neural network and the latter articles deal free energy of a system in a more general level. In short, the results can be interpreted as follows: 1) With TMS, we do work to change the state of the brain, which can be seen in MSS. 2) The brain minimizes the locally high free energy due to work done by TMS, which can be seen as increased SV.

The second interesting observation was that MSS and SV seemed to vary depending on the stimulation parameters. With appropriate paired pulses, we were able to induce a larger MSS at the group level. The larger shift was also followed by

[7]If the studied time intervals have N data points, MSS is an average of N^2 signal-space distances. If we assume that each distance has a noise component independent of the real distance, than the contribution of noise is proportional to $\sqrt{N^2} = N$.

increased SV. This can be looked at also in the context of state dependence. With an appropriate conditioning pulse, we already modified the state of the brain to be more reactive to the actual test pulse. This was seen as an increased post-TMS SV. However, it remains unclear to what extent changes in SV or MSS in different conditions were due to differences in the primary cortical activation caused by TMS, and what was the contribution of the feedback signals resulting from larger MEPs.

All in all, we introduced two novel quantitative tools that were able to characterize dynamic differences between spontaneous and TMS-modulated activity. Furthermore, at the group level, MSS was able to distinguish between stimulation with different effectiveness. MSS and SV might help us better understand the mechanisms of TMS and combined TMS–EEG method in general. Furthermore, they could be easily applied to some other ERP studies where the method to change $\mathbf{J}^{\mathrm{p}}(\mathbf{r})$ would differ from TMS. On the other hand, the connection between the brain state and the EEG signal space is completely analogous to magnetoencephalography (MEG) signal space (Ilmoniemi and Williamson, 1987; Uusitalo and Ilmoniemi, 1997), only the lead field presented in Eq. 4 would be different. Thus, SV and MSS would be directly applicable to MEG data. Based on our results, RQA tools seem promising in studying the brain dynamics in general.

5.2 Inducing facilitation in the cortex

The observed changes in MEPs can be considered a reliable indication of SICF. Hence, in this context, it is well justified to study implications of cortical facilitation in EEG. Indeed, by using EMM, it seemed that also the EEG signal showed the observed facilitation. Our result nicely supports the findings of Fitzgerald et al. (2008, 2009); Daskalakis et al. (2008); Farzan et al. (2008, 2010). To the best of our knowledge, this is the first time when SICF elicited with the specific parameters (an ISI of 5 ms and intensities of 100% of RMT) has been shown using EEG. Furthermore, EMM has previously only been used to quantify intracortical inhibition. Our results indicate that it can be used to measure also facilitation.

Again, the major problem with the results is that although we can observe correlation between the MEP amplitudes and EMM, it is difficult to determine the causal relations. Although EMM would reflect increased cortical excitement it is impossible to say how much the MEP-related somatosensory signals affect these results. Hence, EMM might be partially just a more sophisticated way of measuring MEP amplitudes. In the future, it would be very interesting to study SICM with TMS–EEG outside the M1 since first, this would not produce MEPs and, second, EMG cannot be used to quantify SICM outside the M1.

Although EMG showed significant facilitation with the ISI of 5 ms, we were not able to induce clear inhibition with the ISI of 3 ms. One reason that might explain this is that we compromised with the stimulation parameters. Our goal was to change responses to the same TMS pulse by only modifying the pre-TMS brain state. However, SICI has been observed more robustly with very high test-pulse intensities whereas SICF is often seen with low test-pulse intensities (*e.g.*, Ilić et al., 2002).

5.3 Changes in GMFA suggest that cortical facilitation is visible in TMS–EEG signal

The analysis of GMFA provided several interesting results. The increased MEPs lead us to presume that cortical excitability was, indeed, facilitated by the 100%-RMT conditioning pulse 5 ms prior to the test pulse. Hence, it seems that increased excitability can be seen in the TMS-evoked EEG signal as an increased GMFA amplitude.

The amplitude modulation of P10 could be particularly interesting, since the earliest components are shown to reflect cortical excitability (Huber et al., 2013). Furthermore, it can be expected that these deflections best describe the immediate primary TMS-elicited activation on the M1. The P10 was significantly increased in all the subjects in the facilitatory condition. Similarly, MEPs were increased in all subjects. This could indicate that the early GMFA peak describes the activation level well. Unfortunately, muscle artifacts were present in all subjects except for S4. Despite the attempts to remove the muscle artifact by using the SSP algorithm (Mäki and Ilmoniemi, 2011), it is impossible to say clearly how much of the artifact signal was left to distort the analysis. It is possible that two strong pulses only 5 ms apart from each other create a stronger twitch in the cranial muscles creating an increased GMFA peak.

Possibly the most convincing change in TMS-evoked EEG responses occurred at ~30 ms after the pulse. Especially after muscle-artifact removal, this deflection should be late enough to stay intact of the muscle artifact. On the other hand, it is early enough to not be contaminated by the coil-click induced auditory response or somatosensory response resulting from the MEPs. Still, there was an observable increase in these deflections in all subjects. Earlier, Mäki and Ilmoniemi (2010) showed that in the studied data there was a statistically significant correlation between the peak-to-peak amplitude of the N15–P30 complex and MEP amplitudes. This result could indicate that P30 reflects the excitation level on the M1, agreeing well with our results.

As mentioned earlier, the subject-level results concerning other deflections were much more ambiguous. In a recent article, Ferreri et al. (2011) showed an increase in P60 when using facilitatory paired pulses (ISI of 11 ms). This supports our findings that also P60 could be enhanced by the conditioning pulse. However, the first feedbacks coming from the peripheral tactile sensations might already distort deflections of this latency.

Also N100 amplitude was clearly increased. Explaining modulation in N100 is especially difficult since this deflection may be contaminated by both the auditory response resulting from the coil click (Nikouline et al., 1999) and the somatosensory feedback from the APB activation. Fortunately, two aspects support the view that the N100 modulation mostly reflected changes in the TMS-elicited cortical activation. First, both Paus et al. (2001) and Nikulin et al. (2003) found in their control measurements that the somatosensory feedback did not contribute effectively to N100. Second, our sham controls showed that the white noise masking was sufficient to block most of the auditory response.

N100 has been associated with inhibitory cortical mechanisms (Nikulin et al., 2003) and the cortical silent period subsequent to TMS (Daskalakis et al., 2008).

Indeed, there is some evidence that larger evoked cortical activation would be followed by more pronounced inhibition (*e.g.*, Orth and Rothwell, 2004; Rogasch et al., 2013). Furthermore, Paus et al. (2001) found a significant correlation between N100 and MEP amplitudes. These findings nicely support our results. On the other hand, Nikulin et al. (2003) did not find any correlation between N100 and the recorded MEP amplitudes.

In addition to the increased amplitudes in the facilitatory condition, also latencies were shortened when the ISI was 5 ms. The latencies of the GMFA peaks were advanced 5 ms, which leads to suspect that many of the deflections reflect partially cortical responses evoked by the conditioning pulse. Thus, it is possible that we are not only measuring the effect of the modulated brain state on the test-pulse evoked EEG responses, *i.e.*, secondary effects of the first pulse, but also the primary activation of the conditioning pulse. Previous TMS–EEG studies have shown similar results. For instance, with an ISI of 12 ms the mean (over subjects) latency of P30 was about 8 ms earlier (Paus et al., 2001). Moreover, at the subject level, many datasets showed latency differences even closer to 12 ms. Also Ferreri et al. (2011) reported decreased deflection latencies although clearly smaller than 11 ms.

6 Conclusion

In this Master's thesis, we showed that it is possible to quantify the immediate effects of TMS on the brain state. It seems that the post-TMS brain activity occupies a slightly different region in the state space than the pre-TMS activity. Furthermore, the TMS-modulated brain activity fluctuates more vigorously than spontaneous activity. Both of these effects seem transient and are able to show also non-linear effects of TMS that do not average over trials. These results were confirmed when studying the data measured specially for this work.

The results also imply that the effect of the current brain state on the TMS-elicited changes in EEG can be quantified using our tools, MSS and SV. When the cortex was excited before the test pulse, the post-TMS SV was increased more. Similarly, MSS seemed to be larger when TMS was more effective in generating MEPs. The reliability of these tools was confirmed using more established EEG measures. The EMM showed facilitation in the 5-ms-ISI condition and the grand-average GMFA was clearly largest in this condition.

Hence, it seems that the cortical excitation level before TMS can be quantified using TMS–EEG data. However, all the used measures, the MSS, SV, EMM, and GMFA showed clear effects only at the group level. Unfortunately, the subject-level data was more ambiguous. In this sense, none of the tools examined here proved out to be superior.

The sham studies suggest that the observed results are not contaminated by the auditory artifact. However, the causal relations between the excitability of the cortex, facilitated MEPs, and changed EEG responses still stay as open questions. Namely, parts of the results presented here might be contaminated by the feedback resulting from the somatosensory input of MEPs.

References

Babloyantz, A. (1991). Evidence for slow brain waves: a dynamical approach. *Electroencephalography and Clinical Neurophysiology* 78, 402–405.

Barker, A. T., Jalinous, R., and Freeston, I. L. (1985). Non-invasive magnetic stimulation of human motor cortex. *The Lancet* 325, 1106–1107.

Bennett, M. H. and Jannetta, P. J. (1980). Trigeminal evoked potentials in humans. *Electroencephalography and Clininical Neurophysiology* 48, 517–526.

Civardi, C., Cantello, R., Asselman, P., and Rothwell, J. C. (2001). Transcranial magnetic stimulation can be used to test connections to primary motor areas from frontal and medial cortex in humans. *NeuroImage* 14, 1444–1453.

Claus, D., Weis, M., Jahnke, U., Plewe, A., and Brunhölzl, C. (1992). Corticospinal conduction studied with magnetic double stimulation in the intact human. *Journal of the Neurological Sciences* 111, 180–188.

Daskalakis, Z. J., Christensen, B. K., Fitzgerald, P. B., Roshan, L., and Chen, R. (2002). The mechanisms of interhemispheric inhibition in the human motor cortex. *The Journal of Physiology* 543, 317–326.

Daskalakis, Z. J., Farzan, F., Barr, M. S., Maller, J. J., Chen, R., and Fitzgerald, P. B. (2008). Long-interval cortical inhibition from the dorsolateral prefrontal cortex: a TMS–EEG study. *Neuropsychopharmacology* 33, 2860–2869.

Di Lazzaro, V., Restuccia, D., Oliviero, A., Profice, P., Ferrara, L., Insola, A., Mazzone, P., Tonali, P., and Rothwell, J. C. (1998). Magnetic transcranial stimulation at intensities below active motor threshold activates intracortical inhibitory circuits. *Experimental Brain Research* 119, 265–268.

Di Lazzaro, V., Rothwell, J. C., Oliviero, A., Profice, P., Insola, A., Mazzone, P., and Tonali, P. (1999). Intracortical origin of the short latency facilitation produced by pairs of threshold magnetic stimuli applied to human motor cortex. *Experimental Brain Research* 129, 494–499.

Eckmann, J.-P., Kamphorst, S. O., and Ruelle, D. (1987). Recurrence plots of dynamical systems. *Europhysics Letters* 4, 973–977.

Esser, S. K., Huber, R., Massimini, M., Peterson, M. J., Ferrarelli, F., and Tononi, G. (2006). A direct demonstration of cortical LTP in humans: a combined TMS/EEG study. *Brain Research Bulletin* 69, 86–94.

Farzan, F., Barr, M. S., Levinson, A. J., Chen, R., Wong, W., Fitzgerald, P. B., and Daskalakis, Z. J. (2010). Reliability of long-interval cortical inhibition in healthy human subjects: A TMS–EEG study. *Journal of Neurophysiology* 104, 1339–1346.

Farzan, F., Barr, M. S., Wong, W., Chen, R., Fitzgerald, P. B., and Daskalakis, Z. J. (2008). Suppression of γ-oscillations in the dorsolateral prefrontal cortex following long interval cortical inhibition: A TMS–EEG Study. *Neuropsychopharmacology* 34, 1543–1551.

Ferrarelli, F., Massimini, M., Sarasso, S., Casali, A., Riedner, B. A., Angelini, G., Tononi, G., and Pearce, R. A. (2010). Breakdown in cortical effective connectivity during midazolam-induced loss of consciousness. *Proceedings of the National Academy of Sciences of the United States of America* 107, 2681–2686.

Ferreri, F., Pasqualetti, P., Määttä, S., Ponzo, D., Ferrarelli, F., Tononi, G., Mervaala, E., Miniussi, C., and Rossini, P. M. (2011). Human brain connectivity during single and paired pulse transcranial magnetic stimulation. *NeuroImage* 54, 90–102.

Fitzgerald, P. B., Daskalakis, Z. J., Hoy, K., Farzan, F., Upton, D. J., Cooper, N. R., and Maller, J. J. (2008). Cortical inhibition in motor and non-motor regions: a combined TMS-EEG study. *Clinical EEG and Neuroscience* 39, 112–117.

Fitzgerald, P. B., Maller, J. J., Hoy, K., Farzan, F., and Daskalakis, Z. J. (2009). GABA and cortical inhibition in motor and non-motor regions using combined TMS–EEG: a time analysis. *Clinical Neurophysiology* 120, 1706–1710.

Friston, K. (2010). The free-energy principle: a unified brain theory? *Nature Reviews Neuroscience* 11, 127–138.

Friston, K., Kilner, J., and Harrison, L. (2006). A free energy principle for the brain. *Journal of Physiology Paris* 100, 70–87.

Hämäläinen, M. S. and Ilmoniemi, R. J. (1994). Interpreting magnetic fields of the brain: minimum norm estimates. *Medical & Biological Engineering & Computing* 32, 35–42.

Hannula, H., Ylioja, S., Pertovaara, A., Korvenoja, A., Ruohonen, J., Ilmoniemi, R. J., and Carlson, S. (2005). Somatotopic blocking of sensation with navigated transcranial magnetic stimulation of the primary somatosensory cortex. *Human Brain Mapping* 26, 100–109.

Hashimoto, I. (1988). Trigeminal evoked potentials following brief air puff: Enhanced signal-to-noise ratio. *Annals of Neurology* 23, 332–338.

Heller, L. and van Hulsteyn, D. B. (1992). Brain stimulation using electromagnetic sources: theoretical aspects. *Biophysical Journal* 63, 129–138.

Hopfield, J. J. (1982). Neural networks and physical systems with emergent collective computational abilities. *Proceedings of the National Academy of Sciences of the United States of America* 79, 2554–2558.

Huber, R., Mäki, H., Rosanova, M., Casarotto, S., Canali, P., Casali, A. G., Tononi, G., and Massimini, M. (2013). Human cortical excitability increases with time awake. *Cerebral Cortex* 23, 1–7.

Ilić, T. V., Meintzschel, F., Cleff, U., Ruge, D., Kessler, K. R., and Ziemann, U. (2002). Short-interval paired-pulse inhibition and facilitation of human motor cortex: the dimension of stimulus intensity. *The Journal of Physiology* 545, 153–167.

Ilmoniemi, R. J. and Kičić, D. (2010). Methodology for combined TMS and EEG. *Brain Topography* 22, 233–248.

Ilmoniemi, R. J., Ruohonen, J., and Karhu, J. (1999). Transcranial magnetic stimulation—a new tool for functional imaging of the brain. *Critical Reviews in Biomedical Engineering* 27, 241–284.

Ilmoniemi, R. J., Virtanen, J., Ruohonen, J., Karhu, J., Aronen, H. J., Katila, T., et al. (1997). Neuronal responses to magnetic stimulation reveal cortical reactivity and connectivity. *NeuroReport* 8, 3537–3540.

Ilmoniemi, R. J. and Williamson, S. J. (1987). Analysis for the magnetic alpha rhythm in signal space. *Society of Neuroscience Abstracts* 13, 46.

Iwanski, J. S. and Bradley, E. (1998). Recurrence plots of experimental data: To embed or not to embed? *Chaos: An Interdisciplinary Journal of Nonlinear Science* 8, 861–871.

Julkunen, P., Säisänen, L., Danner, N., Niskanen, E., Hukkanen, T., Mervaala, E., and Könönen, M. (2009). Comparison of navigated and non-navigated transcranial magnetic stimulation for motor cortex mapping, motor threshold and motor evoked potentials. *NeuroImage* 44, 790–795.

Kähkönen, S., Wilenius, J., Nikulin, V. V., Ollikainen, M., and Ilmoniemi, R. J. (2003). Alcohol reduces prefrontal cortical excitability in humans: a combined TMS and EEG study. *Neuropsychopharmacology* 28, 747–754.

Karabanov, A. N., Chi-Chao, C., Paine, R., and Hallett, M. (2013). Mapping different intra-hemispheric parietal-motor networks using twin coil TMS. *Brain Stimulation* 6, 384–389.

Koch, G., Ruge, D., Cheeran, B., Fernandez Del Olmo, M., Pecchioli, C., Marconi, B., Versace, V., Lo Gerfo, E., Torriero, S., Oliveri, M., Caltagirone, C., and Rothwell, J. C. (2009). TMS activation of interhemispheric pathways between the posterior parietal cortex and the contralateral motor cortex. *The Journal of Physiology* 587, 4281–4292.

Komssi, S., Aronen, H. J., Huttunen, J., Kesäniemi, M., Soinne, L., Nikouline, V. V., Ollikainen, M., Roine, R. O., Karhu, J., Savolainen, S., and Ilmoniemi, R. J. (2002). Ipsi- and contralateral EEG reactions to transcranial magnetic stimulation. *Clinical Neurophysiology* 113, 175–184.

Komssi, S., Kähkönen, S., and Ilmoniemi, R. J. (2004). The effect of stimulus intensity on brain responses evoked by transcranial magnetic stimulation. *Human Brain Mapping* 21, 154–164.

Komssi, S., Savolainen, P., Heiskala, J., and Kähkönen, S. (2007). Excitation threshold of the motor cortex estimated with transcranial magnetic stimulation electroencephalography. *NeuroReport* 18, 13–16.

Koponen, L. (2012). Practical limitations of TMS-coil focality. *Special Assignment, Aalto University School of Science.*

Kujirai, T., Caramia, M. D., Rothwell, J. C., Day, B. L., Thompson, P. D., Ferbert, A., Wroe, S., Asselman, P., and Marsden, C. D. (1993). Corticocortical inhibition in human motor cortex. *The Journal of Physiology* 471, 501–519.

Lehmann, D. and Skrandies, W. (1980). Reference-free identification of components of checkerboard-evoked multichannel potential fields. *Electroencephalography and Clinical Neurophysiology* 48, 609–621.

Lioumis, P., Kičić, D., Savolainen, P., Mäkelä, J. P., and Kähkönen, S. (2009). Reproducibility of TMS—Evoked EEG responses. *Human Brain Mapping* 30, 1387–1396.

Mäki, H. (2011). *Studying the Cortical State with Transcranial Magnetic Stimulation.* Aalto University, Doctoral Dissertations.

Mäki, H. and Ilmoniemi, R. J. (2010). The relationship between peripheral and early cortical activation induced by transcranial magnetic stimulation. *Neuroscience Letters* 478, 24–28.

Mäki, H. and Ilmoniemi, R. J. (2011). Projecting out muscle artifacts from TMS-evoked EEG. *NeuroImage* 54, 2706–2710.

Malmivuo, J. and Plonsey, R. (1995). *Bioelectromagnetism: Principles and Applications of Bioelectric and Biomagnetic fields.* Oxford University Press, USA.

Malmivuo, J., Suihko, V., and Eskola, H. (1997). Sensitivity distributions of EEG and MEG measurements. *IEEE Transactions on Biomedical Engineering* 44, 196–208.

Marwan, N., Carmen Romano, M., Thiel, M., and Kurths, J. (2007). Recurrence plots for the analysis of complex systems. *Physics Reports* 438, 237–329.

Massimini, M., Ferrarelli, F., Huber, R., Esser, S. K., Singh, H., and Tononi, G. (2005). Breakdown of cortical effective connectivity during sleep. *Science* 309, 2228–2232.

Massimini, M., Ferrarelli, F., Murphy, M. J., Huber, R., Riedner, B. A., Casarotto, S., and Tononi, G. (2010). Cortical reactivity and effective connectivity during REM sleep in humans. *Cognitive Neuroscience* 1, 176–183.

Mochizuki, H., Huang, Y.-Z., and Rothwell, J. C. (2004). Interhemispheric interaction between human dorsal premotor and contralateral primary motor cortex. *The Journal of Physiology* 561, 331–338.

Morishima, Y., Akaishi, R., Yamada, Y., Okuda, J., Toma, K., and Sakai, K. (2008). Task-specific signal transmission from prefrontal cortex in visual selective attention. *Nature Neuroscience* 12, 85–91.

Mutanen, T., Mäki, H., and Ilmoniemi, R. J. (2013). The effect of stimulus parameters on TMS–EEG muscle artifacts. *Brain Stimulation* 6, 371–376.

Mutanen, T., Nieminen, J. O., and Ilmoniemi, R. J. (2013). TMS-evoked changes in brain-state dynamics quantified by using EEG data. *Frontiers in Human Neuroscience* 7, 155.

Nikouline, V., Ruohonen, J., and Ilmoniemi, R. J. (1999). The role of the coil click in TMS assessed with simultaneous EEG. *Clinical Neurophysiology* 110, 1325–1328.

Nikulin, V. V., Kičić, D., Kähkönen, S., and Ilmoniemi, R. J. (2003). Modulation of electroencephalographic responses to transcranial magnetic stimulation: evidence for changes in cortical excitability related to movement. *European Journal of Neuroscience* 18, 1206–1212.

Orth, M. and Rothwell, J. C. (2004). The cortical silent period: intrinsic variability and relation to the waveform of the transcranial magnetic stimulation pulse. *Clinical Neurophysiology* 115, 1076–1082.

Ouyang, G., Li, X., Dang, C., and Richards, D. A. (2008). Using recurrence plot for determinism analysis of EEG recordings in genetic absence epilepsy rats. *Clinical Neurophysiology* 119, 1747–1755.

Paus, T., Sipila, P. K., and Strafella, A. P. (2001). Synchronization of neuronal activity in the human primary motor cortex by transcranial magnetic stimulation: an EEG study. *Journal of Neurophysiology* 86, 1983–1990.

Pijn, J. P. M., Velis, D. N., van der Heyden, M. J., DeGoede, J., van Veelen, C. W. M., and da Silva, F. H. L. (1997). Nonlinear dynamics of epileptic seizures on basis of intracranial EEG recordings. *Brain Topography* 9, 249–270.

Rogasch, N. C., Daskalakis, Z. J., and Fitzgerald, P. B. (2013). Mechanisms underlying long-interval cortical inhibition in the human motor cortex: a TMS–EEG study. *Journal of Neurophysiology* 109, 89–98.

Uusitalo, M. A. and Ilmoniemi, R. J. (1997). Signal-space projection method for separating MEG or EEG into components. *Medical and Biological Engineering and Computing* 35, 135–140.

Valls-Solé, J., Pascual-Leone, A., Wassermann, E. M., and Hallett, M. (1992). Human motor evoked responses to paired transcranial magnetic stimuli. *Electroencephalography and Clinical Neurophysiology/Evoked Potentials Section* 85, 355–364.

Van Der Werf, Y. D. and Paus, T. (2006). The neural response to transcranial magnetic stimulation of the human motor cortex. I. Intracortical and cortico-cortical contributions. *Experimental Brain Research* 175, 231–245.

Virtanen, J., Ruohonen, J., Näätänen, R., and Ilmoniemi, R. J. (1999). Instrumentation for the measurement of electric brain responses to transcranial magnetic stimulation. *Medical and Biological Engineering and Computing* 37, 322–326.

Wassermann, E., Epstein, C., and Ziemann, U. (2008). *Oxford Handbook of Transcranial Stimulation.* Oxford University Press.

Ziemann, U., Tergau, F., Wassermann, E. M., Wischer, S., Hildebrandt, J., and Paulus, W. (1998). Demonstration of facilitatory I wave interaction in the human motor cortex by paired transcranial magnetic stimulation. *The Journal of Physiology* 511, 181–190.